FOURTH ANNUAL CONFERENCE

AMERICAN SOCIETY OF BIOMECHANICS

University of Vermont

Radisson Hotel

Burlington, Vermont

October 9 - 10, 1980

PHYSIOLOGICAL PERIODS: EFFECTS OF SCALE

Thomas A. McMahon
Gordon McKay Professor of Applied Mechanics
Harvard University
Cambridge, MA 02138

Many periods or characteristic times in animal physiology are found to be proportional to the 1/4 power of animal body weight. These include breath period, heart period, the period characterizing the first impedance minimum of the arterial system, the time constant for elastic recoil of the lung, and the time constant for clearance of drugs from the plasma. An argument is developed to account for these observations, based on elastic similarity between animals of different body size.

TRENDS IN SKIING INJURIES

R. Johnson, M.D. - University of Vermont, Burlington, Vermont

The skiing population and injuries at Sugarbush North ski area in Vermont were monitored from 1972 through 1978. Over this time, 407,604 skier visits were accrued and 1,711 injuries were sustained. A clinic in the base lodge was staffed full-time by orthopaedic surgeons and technicians. In addition to medical diagnosis, treatment and questioning of injured skiers, a detailed study of their equipment function was also performed. A control population (999 skiers) was selected at random for identical study. We made over 11,000 parking lot interviews and ski rack samples to be certain that our control population truly represented the average population skiing at the mountain.

A goal of this on-going study is to identify the high-risk group of the skiing population and to determine if modern equipment and procedures can reduce this risk. Although the attempt to determine the precise causes and prevention of specific skiing injuries is still underway, significant trends for specific groups of injuries are already apparent. These trends were measured using regression analysis with an exponential curve, which best fits this relationship.

Over the six-year period, the general injury rate has dropped 41% (r^2= .49, $p > .1$). Upper body injuries are down only 25% (r^2= .12, $p > .1$), but lower extremity injuries are down 50% (r^2= .76, $p < .025$). Adjusting for age and sex to a standard six-year composite population showed an even greater significance for the lower extremity injuries, but again the upper body decrease in rate was not significant. Among the specific lower extremity subgroups, ankle sprains were down 71% (r^2= .80, $p < .025$), and tibial fractures were down 74% (r^2= .72, $p < .05$). Other groups such as knee sprains showed only a modest reduction of 34% (r^2= .47, $p > .1$).

When injuries which occurred below the knee and could have been caused by the ski acting as a lever to bend or twist the leg were grouped, the reduction in rate was 56% (r^2= .83, $p < .025$). The subgroup of injuries due primarily to twist have dropped by 67% (r^2 =.92, $p < .005$), but injuries due to bending (boot-top tibial and fibular fractures, boot-top contusions and heel cord ruptures) have dropped only 39% (r^2= .43, $p > .1$). Thus protection from these bending injuries may require improvements in both boot and binding design.

The strong correlation between specific lower extremity injuries and time supports a reduction attributable to improvements in equipment technology. These findings do not suggest the dramatically reduced lower extremity rates are explained entirely by improved instructions, snow conditions, trail grooming, and other trail-related factors, as upper body injuries show no statistically significant decrease in the same period.

Because knee sprains have not declined as rapidly as tibial fractures and ankle sprains more emphasis must be placed on better understanding of the mechanisms of knee sprains and the development of equipment and procedures to prevent them. An increase in the relative frequency of properly functioning equipment is primarily responsible for the decline in LEER injuries. Although the relative frequency of properly adjusted bindings is increasing, more than one-half of the equipment in use is still set higher than recommended.

For Presentation at Fourth Annual Conference of

the American Society of Biomechanics,

October 10, 1980

FUNCTIONAL ANTHROPOMETRY - A BASIS FOR BIOMECHANICS OF THE HUMAN BODY

by

K.H.E. Kroemer
Professor and Director, Ergonomics Laboratory
Wayne State University, Detroit, MI 48202

Largely based on the results of the recent Symposium on "Anthropometry and Biomechanics" (July 1980, Cambridge, England), this paper summarizes the current status of engineering anthropometry. It indicates sources of anthropometric data needed by the biomechanical engineer. It discusses the practical application of anthropometric information to the modelling and design of manned systems for optimal fit to the human, for highest safety, and best performance. It also indicates techniques for design evaluation, and for the procurement of additional anthropometric data.

Applied Research in Sports Biomechanics: Performance Characteristics of World-Class Cross-Country Skiers

by

Charles J. Dillman
University of Illinois

The purpose of this presentation is to illustrate how relatively simple biomechanical analyses can make a significant contribution to the understanding of a sports activity. At the request of the National Coaching Staff of the United States Cross-Country Ski Team, an applied biomechanical analysis was conducted to determine the significant technique differences between American and European cross-country skiers. High-speed films were taken of five races during the 1979 Pre-Olympic competition which were held in Lake Placid, New York. Three to four camera sites were utilized every race to film both male and female world-class cross-country skiers in order to maximize the number of performance samples for this select group of skiers. In addition, a time interval investigation was conducted for two races to provide continuous performance data on every skier. The timing data served to validate and support the biomechanical results.

Initial analysis centered around the relationship between the stride variables of length and rate with skiing velocity. For the diagonal stride on a relatively flat terrain, stride length was found to be significantly correlated with velocity for both men and women skiers. Fatigue did not seem to affect these basic relationships. Similar findings were also found for uphill skiing, in that stride length seemed to be the most significant variable that was related to skiing velocity. Analysis within a stride indicated that differences in stride length could be accounted for in the three basic phases of the stride. These phases were the kick, glide, and poling. Statistical analysis of other performance factors indicated, in general, that the trunk was placed at a greater degree of flexion throughout the stride for those who were the better performers. The resultant force of the kick or leg work phase seemed to be directed more in line with the desired path of motion for those skiers that exhibited a longer stride length. During the glide phase, those skiers who had longer stride lengths positioned the body more towards the rear of the ski to facilitate the gliding of the ski in the track. The highly-skilled skiers exhibited a distinct poling style which was characterized by a more forward and vertical pole plant and were able to maintain the movement of the ski in the track throughout the poling phase. These findings indicated that there were some significant technique adjustments that should be made by American skiers to increase their stride length and, consequently, increase their speed of skiing. Associated with these technique changes has to be a re-emphasis in training upon simulating actual competition speeds using the technique adjustments that were recommended. This study has indicated that relatively simple biomechanical analyses can provide meaningful information for the practitioner.

Philip M. Lintilhac. Dept. of Botany, The University of Vermont. Burlington, Vt. 05405

The Role of Mechanical Stress in the Control of Plant Growth and Development.

This paper concerns the effects of mechanical stress on the behavior of plant cells and tissues. Although most other work on this topic is directed at an understanding of mechanical stresses of external origin, namely wind and vibrational stresses, our emphasis is upon mechanical stresses of internal origin, in that we are concerned with stress conditions which arise in a growing tissue because of the growth and development of the tissues themselves. These stresses, which one might term growth stresses, may serve as an epigenetic developmental control system which determines the orientation of new cell partitions as they are installed in an actively dividing tissue, thereby directly determining the final form of the growing organ. Furthermore, since these "Locked-in-stresses" are severely altered or lost when a portion of a plant tissue is explanted for culture in vitro, the behavior of the explanted tissues is correspondingly altered and frequently results in the loss of the plant's ability to undergo normal morphogenesis in vitro, producing only an amorphous "Callus".

In botanical terms, one of the most universal observational truths which is still unexplained is the ubiquitous formation of branch buds in the "Axil" of a leaf. Branches always originate at the point of attachment of the leaf to the stem. At the stage when the location of branch buds is being determined the subtending leaf is just a cellular protuberance on the growing apex; nevertheless we feel that the growth stresses which arise in the tissue interact with this primordial bump, forming a stress concentration in the axil - the notch formed where the bump attaches to the growing apex. Thus we see the areas of commonality of plant morphogenesis as being due to the universal ability of plant cells to respond predictably to mechanical stress. Plant cells apparently have an internal mechanism whereby they can "See" the principal stresses propagating through a tissue; even though such a cell is in part a hydrostatic structure. This unknown mechanism is what results in a plant cell's ability to install a new division wall in a shear-free-plane, perpendicular to one of the principal stresses. We have studied these questions using simple photoelastic models and have confirmed that the cell wall patterns do in fact tend to conform to the stress patterns generated by our models, even though our abilities to reproduce in vivo loading conditions are most primitive.

Lintilhac, P. M. and T. B. Vesecky. 1980 Mechanical Stress and Cell Wall Orientation in Plants. II. Photoelastic Derivation of Principal Stresses in a Model. With a Discussion of the Concept of axillarity and the significance of the "Arcuate Shell Zone". Am. Jnl. Bot. Vol 66. In Press.

FEEDING AT LOW REYNOLDS NUMBER: PARTICLE CAPTURE BY COPEPODS

M. A. R. Koehl
Department of Zoology, University of California, Berkeley, California 94720

Calanoid copepods are abundant planktonic crustaceans that play a major role in the transfer of energy through marine food chains. Many calanoid copepods feed on particulate food (such as diatoms and flagellates) and have been described as "filter feeders". In spite of the ecological importance of copepod feeding, the mechanisms by which these animals capture particles has been poorly understood. The purpose of this investigation was to study copepod feeding mechanisms by elucidating the water motions produced by various actions of their feeding appendages.

High-speed (500 frames$\cdot s^{-1}$) movies were made (in collaboration with J.R. Strickler, who designed the optical set-up) of feeding Eucalanus pileatus. By marking water near the copepods with ink released from a micropipette, I have been able to analyze the feeding currents of these animals (diagrammed below). Copepods are not filterers as they have been described in textbooks, but rather propell water past themselves by flapping their feeding appendages and actively capture small parcels of that water that contain food particles by flinging and closing their second maxillae.

The feeding mechanisms of copepods can be best understood if the process is considered in terms of the physical world of these tiny animals. Because copepods are small (the E. pileatus studied were <1.5mm long), their physical world is dominated by viscous forces rather than the inertial forces that large organisms like humans encounter when moving through fluids. The bristles (setae) on the tips of various feeding appendages attain maximum velocities of 5 - 60 mm$\cdot s^{-1}$ and operate at maximum Reynolds numbers of only 2×10^{-2} to 2×10^{-1} (Reynolds number, which is the ratio of inertial to viscous forces for a flow situation, is given by $\rho VL/\mu$, where V is the relative velocity of a fluid across a solid object, L is a linear dimension of the object, and ρ is the density and μ the viscosity of the fluid). In the viscous world of a copepod, water flow is laminar, bristly appendages behave as solid paddles rather than open rakes, particles can neither be scooped up or left behind because appendages have thick layers of water stuck to them, and water and particle movement stops immediately when an animal stops beating its appendages.

This study, which reveals how copepods move water to capture food particles, illustrates the importance of considering the physical forces which are most important at the size scale of the organisms being studied.

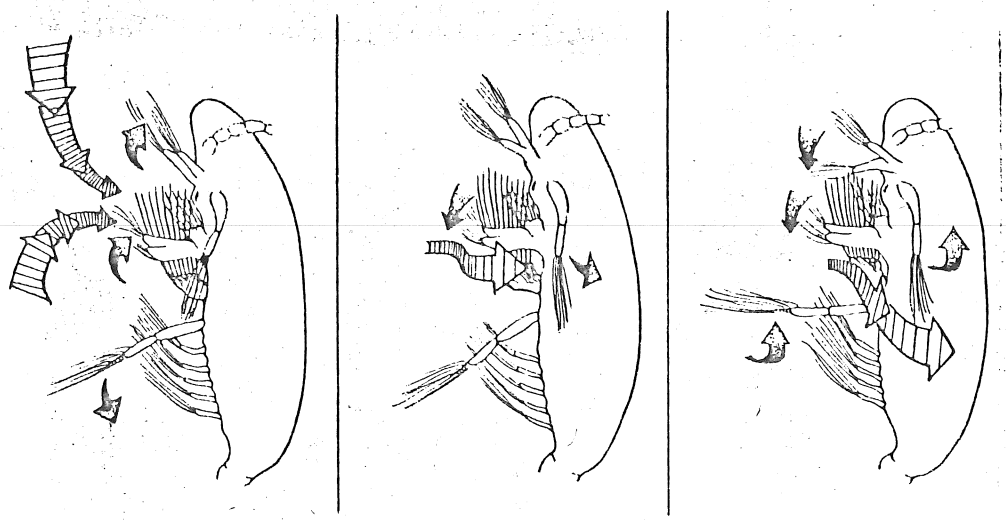

Diagrams of feeding appendage movements (stippled arrows) and the water motion (striped arrows) they produce during one cycle of flapping of an E. pileatus. Appendages beat at 15 - 25 Hz.

Some Recent Results on Growth Stresses in Trees

Robert R. Archer
Department of Civil Engineering
University of Massachusetts
Amherst, MA 01003

The first systematic measurements of growth stresses in trees were made about 40 years ago in Australia. In recent years, new methods have yielded details as to both longitudinal and circumferential surface distributions, as well as internal residual stress patterns.

The strains induced during the development of each new growth layer at the periphery gives rise to increments of residual stress in the interior. Continuum models have been derived to explain the longitudinal, radial, and tangential residual stress distributions found in the interior of logs.

Reorientation of stems and branch movements are associated with growth stress patterns leading to recovery movements. So called tension wood (TW) and compression wood (CW) cells develop in response to particular stimuli and modify the normal growth strain level toward higher tension (TW) or compression (CW).

VISCOELASTIC PROPERTIES OF CONNECTIVE TISSUE FROM CHICKENS WITH SCOLIOSIS

Cutler, A.D.*, Riggins, R.S., Lin, H.J., Ramey, M.R.**, Herrmann, L.R.**
Dept. Orthopaedics, University of California, Davis, 4301 "X" St., Sacramento, California 95817

Previous studies of an inbred line of chickens which develop idiopathic scoliosis indicated the disorder was associated with a connective tissue defect as the animals exhibited increased collagen solubility[1]. Furthermore, chickens that develop scoliosis have abnormally high levels of hydroxyproline in their plasma. This report is concerned with the viscoelastic properties of the tendons and spinal ligaments from these scoliotic chickens.

METHODS AND MATERIALS

Eleven chickens from the scoliotic strain and eighteen from a closely matched hyline strain (Comstock) provided the material. Age range was 10-20 weeks and weight from 1.3 - 1.5 kg. Because of the smaller size of the scoliotic chickens, the controls tended to be slightly younger. Flexor and extensor tendons were removed from the legs and stored in chick serum at -20 degrees F, until testing. Similarly, the mobile spinal segment T5-T6 was removed preserving the ligamentous attachments between the two vertebra and stored until testing.

Tests were performed with an Instrom. For the tendons an initial strain of 4% was applied in 1 to 1.5 sec and observed for 1000 sec. The force time curve was plotted on an x-y recorder. For the spinal ligaments it was not possible to apply a fixed initial displacement, therefore a fixed initial force of 3 kg was applied. From previous experience this force represented less than 1/3 the ultimate force required to disrupt the ligaments.

RESULTS

The results from testing the tendons were linear when plotted on Log normal paper. The mean slopes were significantly different at $p < 0.01$ (Fig. 1). For the spinal ligaments, the results plotted on Log Log paper were linear and the slopes were also significantly different at $p < 0.05$ (Fig. 2).

CONCLUSIONS

The above study indicates that chickens from an inbred line that develop idiopathic scoliosis not only exhibit abnormalities in the metabolism of their connective tissue but also mechanical differences as well. These findings may be related to the etiology of the scoliosis.

Riggins, R.S., Abbott, U.K., Ashmore, C.R., Rucker, R.B. and McCarrey, J.R.: Scoliosis in Chickens, J. Bone and Joint Surg. 59-A(8):1020-1026, 1977.

*Boeing Aircraft, Seattle, Washington
**Dept. Civil Engineering, University of California, Davis, Davis, California 95616

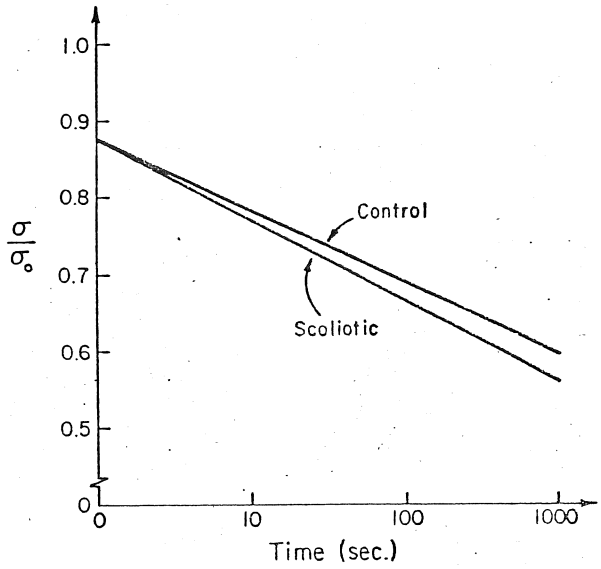

Fig. 1 - Plot of Mean Results of Tendon Stress Relaxation Tests.

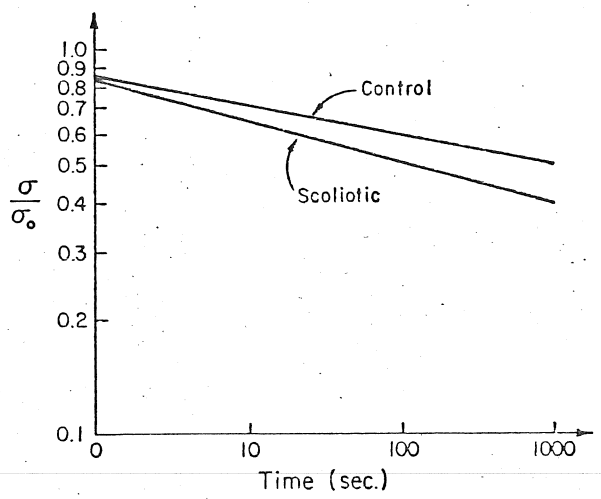

Fig. 2 - Plot of Mean Results of Spinal Stress Relaxation Tests.

4301 "X" Street, Sacramento, Calif. 95817

STRAIN MEASUREMENT IN THE MEDIAL COLLATERAL LIGAMENT

John Boyle
Steven Arms
Robert Johnson
Malcolm Pope

Purpose: In evaluating and treating injuries to the medial collateral ligament (MCL) of the knee it is important to know the ligament strain characteristics with respect to joint position and force application. Previous studies have shown a wide variety of findings. The intention of this study is to accurately "map" absolute strain in the MCL as a function of joint angle and then to record changes in strain pattern with the application of forces about the knee, i.e. abduction, external rotation.

Methods: We have developed a sensitive transducer for measuring strain. This device employs a tiny magnetic field sensing device to detect the linear displacement of a .5mm diameter magnetic core within a slightly larger diameter tube. The transducer is accurate to .001" and can be attached to the ligament with a minimal amount of influence on its physiologic behavior. Output from the device is amplified and plotted on the Y-axis of an X-Y recorder.

The initial phase of investigation was carried out using 5 amputation specimens. Each knee was fixed at its tibial end to an apparatus which permits normal range of motion and the application of forces. A potentiometer recorded flexion angle which was plotted on the X-axis.

The transducer was attached to 5 well defined areas on the MCL of each specimen. Motion through a range of 0^{o} (full extension) to 120^{o} was carried out and followed with the application of known abduction forces on the femur. A strain "map" of each ligament as function of joint position both with and without abduction force was obtained.

Results: Strain in the anterior long fibers (ALF) increased slightly as the knee was flexed to 90^{o} after which it decreased rapidly. Posterior long fibers (PLF) began to relax immediately after flexion and continued to 120^{o}. Posterior oblique fibers (POF) behaved in similar fashion but showed a greater degree of relaxation. Strain in both ALF and PLF never exceeded 2.5%. Application of a valgus force in extension caused no change in strain but readings dramatically increased especially in ALF as the knee was put into flexion.

Instrumentation of fresh cadaver knees is currently in progress in an attempt to obtain more meaningful data. Plans to measure MCL strain *in vivo* are under consideration.

This study will provide better insight to normal knee ligament biomechanics as well as to the mechanism and treatment of MCL injuries. The current literature is replete with conflicting opinions about ligament strain characteristics and this new method of measuring strain should help to solve some of this controversy.

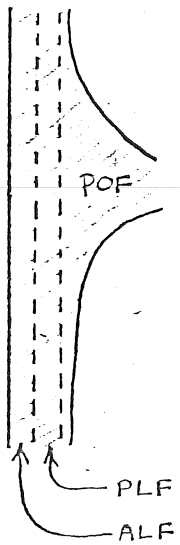

Department of Orthopaedic Surgery
University of Vermont College of Medicine
Burlington, Vermont 05405

A MODEL OF CUMULATIVE TRAUMA DISORDERS IN TENDONS AND TENDON SHEATHS

S.A. Goldstein*
T.J. Armstrong**
D.B. Chaffin ***

Tendon and tendon sheath disorders, such as tenosynovitis, tendonitis, synovitis, deQuervain's disease, and others are associated with repetitive forceful exertions of the hands and wrists. This paper describes a biomechanical model for investigations of the etiology of these disorders.

A viscoelastic model in which stress in the tendon and tendon sheaths is related to specific patterns of hand and wrist exertions is proposed. Strain response of the tendon-tendon sheath composite is described with respect to variations in magnitude, frequency and duration of hand exertions. Injury to the tendon, tendon sheath, and trochlea structures is characterized by cumulative strain or creep in response to repetitive loading. Degeneration of normal gliding function, associated with tissue microfailure, fatigue failure, or compromises in nutrient supplies, is theorized.

This model is supported by pilot studies of the viscoelastic properties of fresh tendon preparations in cadaver hands. The figure below illustrates stress relaxation during repeated application of physiological loads at 0.22 cycles/sec.

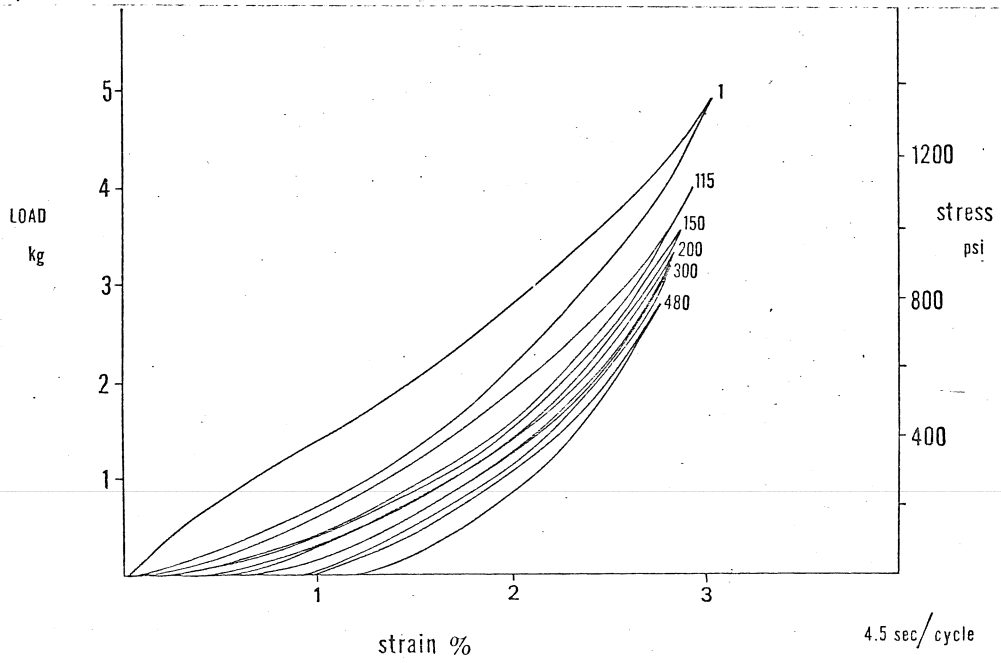

Response of unembalmed FDS tendon in cadaver hand to cyclic loading to constant strain.

* Bioengineering, The University of Michigan , Ann Arbor, MI 48109
** Environmental and Industrial Health, The University of Michigan
*** Industrial and Operations Engineering, The University of Michigan

THE MECHANICS OF HORSE LOCOMOTION: STRAINS DEVELOPED IN THE LIMB BONES AT DIFFERENT GAITS.

Biewener, Andrew A., Thomason, Jeff[+], Goodship, A.E.[*] & Lanyon, L.E.[*]

Museum of Comparative Zoology, Harvard University, Cambridge, Mass.
[+]Dept. of Zoology, University of Toronto, Toronto, Canada
[*]Dept. of Veterinary Anatomy, University of Bristol, Bristol, England

Ground contact forces and limb bone loading were measured simultaneously in vivo from bone bonded strain gauge rosettes and force plate recordings from three adult horses walking, trotting and cantering at different speeds. The rosettes were attached to the cranial(dorsal) and caudal(palmar/plantar) cortices of the midshaft on the radius, metacarpus, tibia and metatarsus.

In the forelimb the peak principal compressive strain($\epsilon_{c\text{-}tot}$) in the caudal cortex of each bone reflects the change in vertical ground force(F_v) with increasing running speed(Fig. 1 A&B). F_v rises from a walk to a fast trot but falls slightly after the trot-canter transition. In the hindlimb bones the peak principal compressive strain ($\epsilon_{c\text{-}tot}$) continues to increase with speed despite a similar leveling off in F_v after the trot-canter transition. The higher strain levels recorded from the radius and tibia, and the metatarsus at higher speeds, are due primarily to increased bending strain(ϵ_b) developed in those bones. The metacarpus, in contrast, shows a fall in ϵ_b from a walk to a fast trot, indicating a more uniform compressive load at higher speeds. The overall strain pattern($\epsilon_{c\text{-}tot}$) is thus more closely associated with changes in F_v.

The correlation in all four bones between axial compressive strain(ϵ_c) and F_v is demonstrated further by the similar rise and plateau after the t-c transition as found in F_v. The compressive force exerted on each bone was calculated from the stress due to the compressive strain(assumed modulus: 18 GN/m^2). At a fast trot values for the radius and tibia, 6447 N ($2.22 \times F_v$) and 4657 N ($2.33 \times F_v$) respectively, compare with those for the metacarpus and metatarsus, 9769 N ($3.31 \times F_v$) and 8306 N ($4.26 \times F_v$) respectively.

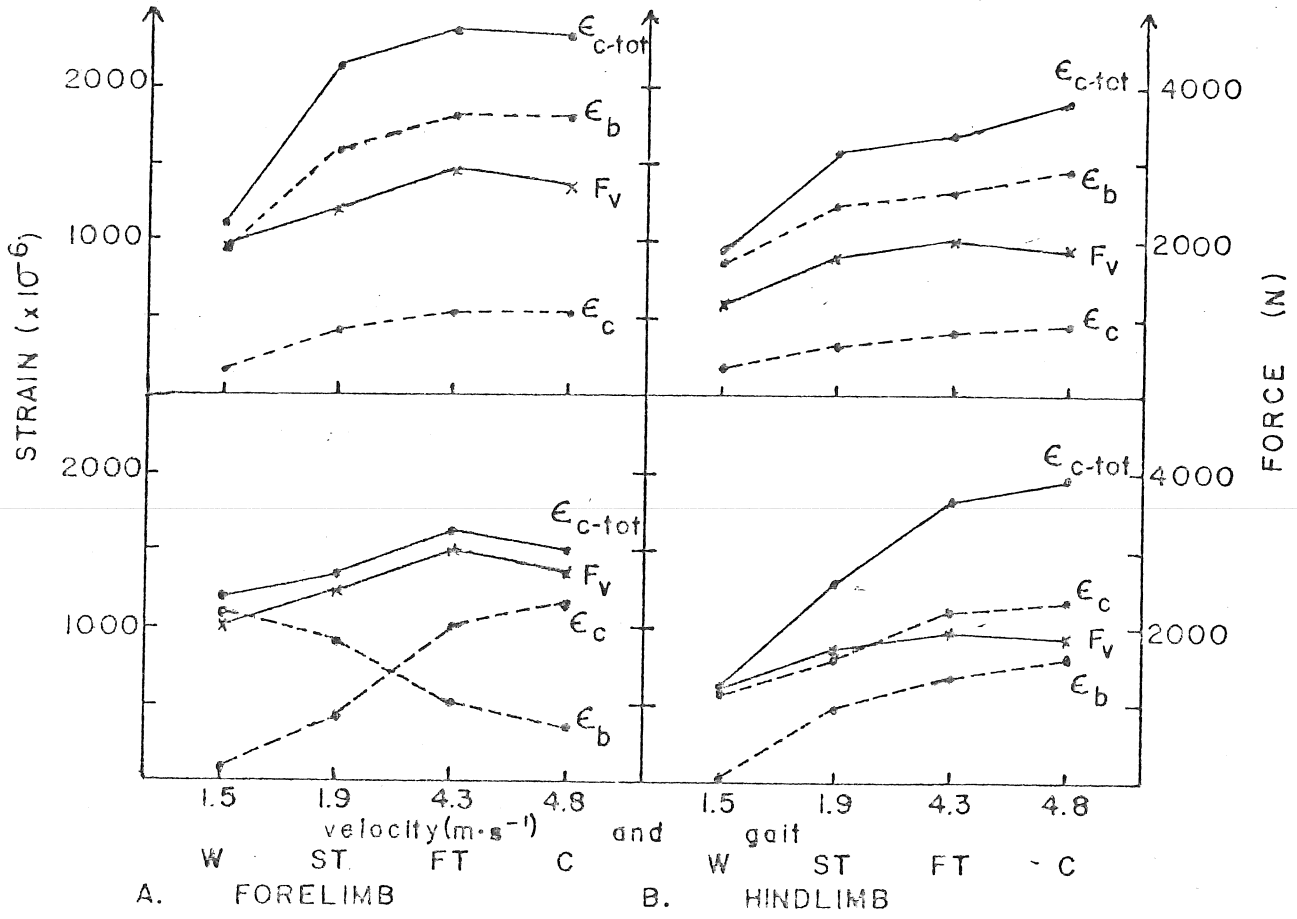

Fig. 1 Graphs of F_v, $\epsilon_{c\text{-}tot}$, and its two components, ϵ_b and ϵ_c, versus gait and running speed for each bone(data from two horses, 281 and 269 kg.).

UNIAXIAL FATIGUE OF HUMAN CORTICAL BONE - THE INFLUENCE OF STRESS RANGE, STRAIN RANGE, AND PHYSICAL CHARACTERISTICS

W.E. Caler, D.R. Carter, (Orthopaedic Research Laboratories, Massachusetts General Hospital, Harvard Medical School, Boston, MA 02114) D.M. Spengler and V.H. Frankel (Department of Orthopaedics, University of Washington, Seattle, WA).

Previous studies of cortical bone fatigue have primarily used rotating-bending tests at high loading frequencies. However, bone fatigue resistance increases with increasing frequency. In addition, bone specimens tested in rotating-bending result in more optimistic estimates of fatigue strength than specimens loaded uniaxially. In this study, a uniaxial loading apparatus and physiologic loading rates were used. The effects of strain range, stress range, mean strain, bone modulus, porosity, density and ash fraction on bone tissue fatigue life were investigated.

Seventy-five devitalized cortical bone specimens were machined from the mid-diaphyses of human femora. Testing was performed on an MTS electrohydraulic testing system under strain control at a strain rate of 0.01. This strain rate corresponds to frequencies of 0.5 to 1.0 Hz for strain ranges ($\Delta\varepsilon$) of 0.010 to 0.005 respectively. Specimens were kept wet at all times and testing was done at 37°C.

Fatigue life was found to be dependent primarily upon cyclic strain range and independent of mean strain. Plots of initial stress range ($\Delta\sigma$) vs. cycles to failure (N_f) exhibited much more data scatter than plots of total strain range ($\Delta\varepsilon$) vs. cycles to failure. Both curves showed positive correlations between fatigue life and specimen modulus, but the correlation of modulus with the $\Delta\sigma$ vs, N_f curve was much stronger, accounting for much of the data scatter. Table I shows the effects of adding modulus as an independent variable to the regression equations; N_f as a function of $\Delta\varepsilon$ and N_f as a function of $\Delta\sigma$. The regression coefficient of modulus in equation 4 is almost 4 times larger than the coefficient of modulus in equation 2. In addition, there is a much more pronounced reduction in the standard error of equation 3 when modulus is added as an independent variable. A weak, negative correlation was found between fatigue life and porosity. Correlations between fatigue life and bone density or ash fraction were not significant.

TABLE I REGRESSION EQUATIONS (S.D.)

1.	$\log N_f$ =	$-5.342 \log \Delta\varepsilon$ (0.544)	-8.532		S.E.E. = 0.4085
2.	$\log N_f$ =	$-4.908 \log \Delta\varepsilon$ (0.539)	$+0.048$ E (0.017)	-8.307	S.E.E. = 0.3882
3.	$\log N_f$ =	$-2.050 \log \Delta\sigma$ (0.686)	$+6.991$		S.E.E. = 0.5990
4.	$\log N_f$ =	$-4.824 \log \Delta\sigma$ (0.527)	$+0.186$ E (0.019)	$+9.914$	S.E.E. = 0.3871

The results reveal a much poorer bone fatigue resistance than has been indicated by previous studies. There was a much stronger dependence of bone fatigue life on strain range than on stress range. Knowledge of the in vivo bone tissue strain history, in addition to knowledge of bone modulus and porosity would facilitate reliable predictions of cortical bone fatigue failure.

Supported by NIH grant AM 27117

STRUCTURAL PROPERTIES OF IMMATURE WHOLE BONE

P. A. Torzilli, K. Takebe*, A. H. Burstein, K. G. Heiple+
Biomechanics Department, The Hospital for Special Surgery
535 East 71 Street, New York, New York 10021

INTRODUCTION

Bending of immature whole bone beyond the elastic limit exhibits non-elastic yielding and permanent deformation without concomitant boney fracture. Mature bone is stiffer, has a substantially decreased amount of non-elastic deformation and does not exhibit permanent angulation after load release. Large non-elastic permanent deformations in immature bone, most often seen in the forearm of children, has been termed "plastic bowing." This phenomena is dependent upon the bone's material properties and cross-sectional geometric properties. Previously (Am. Soc. Biomechanics, 1979) we reported on the material properties of immature canine bone. The linear and non-linear stress and moduli were found to increase with age, while the strain was independent of age. This investigation is concerned with the variation with age in the whole bone bending properties of maturing canine bones.

MATERIALS AND METHODS

Paired femora and tibia were obtained from 22 Labradors ranging in age from one week to adult. Total length and cross-sectional properties were determined for each bone. Three and four point bending tests were performed to determine each bone's stiffness, yield strength, maximum bending moment and total amount of permanent deformation after load release.

RESULTS

Bending tests showed that all bones exhibited an initial linear region followed by a large region of non-elastic deformation. Stiffness increased with maturity while non-linear deformation decreased substantially. In the youngest bones large permanent deformations were noted upon load release, with decreasing amounts of permanent deformation occurring with maturity. In all bones the structural rigidity increased with age, indicating a greater ability to carry load. A typical set of results for the tibia in four point bending are shown below.

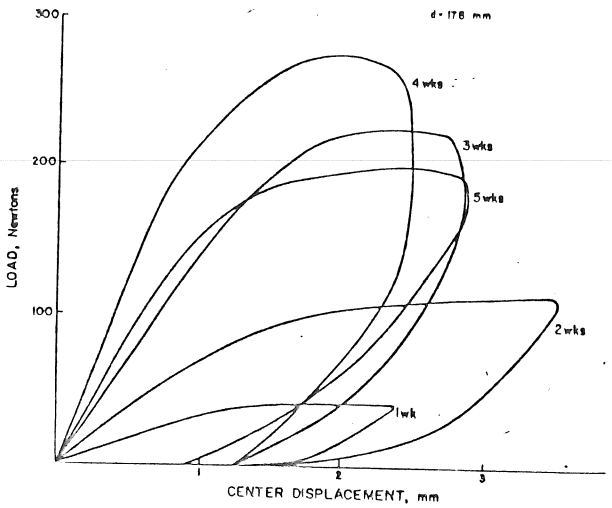

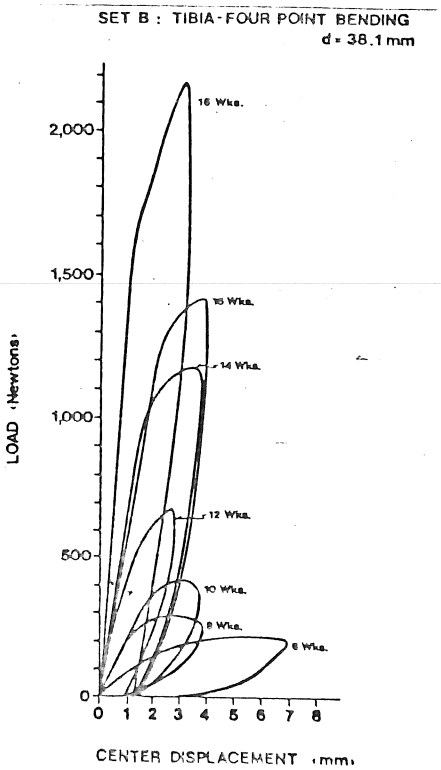

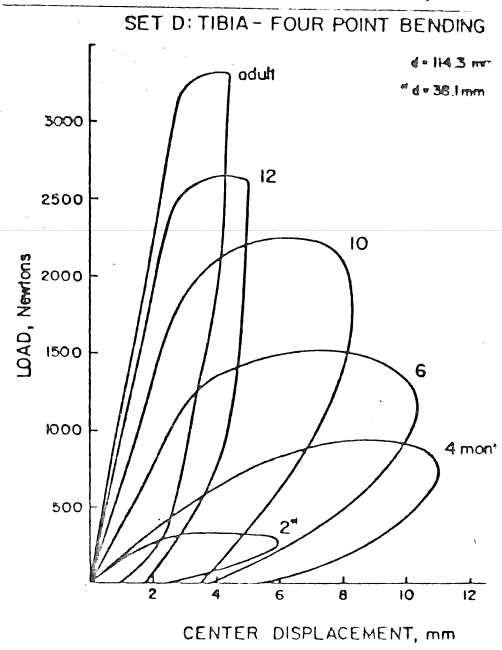

AGE AND SEX DIFFERENCES IN GEOMETRICAL PROPERTIES OF THE HUMAN FEMUR AND TIBIA

C.B. Ruff and W.C. Hayes
Orthopaedic Biomechanics Laboratory
Beth Israel Hospital and Harvard Medical School
330 Brookline Avenue
Boston, MA. 02215

Several authors have used radiographic measurements to suggest age related remodeling of long bone cortices. Detailed geometric analyses of long bone cross-sections have previously been limited in sample size due to the time consuming nature of manually tracing and inputing cross-section coordinates. Because of the large amount of normal inter-individual variation in bone cross-sectional geometry, large sample sizes are necessary if sex and age differences are to be clearly delineated.

Using a digitizer and interactive computer software (Nargurka and Hayes, 1980), section properties (areas, centroid coordinates, principal moments and their orientations) of 1320 femoral and tibial cross sections were determined and analyzed statistically for sex and age differences. Specimens were obtained from the Pecos Archaeological collection (Harvard Peabody Museum), and included 60 males and 60 females equally divided between 6 adult age groups. Femora and tibiae were sectioned, photographed and analyzed at 5 diaphyseal sites and at 1 site through the femoral neck.

Although individuals within sex and age groupings displayed variability in cross-sectional geometry, some clear sex and age-related trends were observed. Males displayed relatively greater A-P oriented areal moments in both the tibia and femur and were relatively larger in mid shaft regions, suggesting adaptation to greater A-P bending moments. With aging, outer dimensions (subperiosteal areas) increased at all cross section locations in both sexes. Subperiosteal expansion largely offset endosteal resorption, with male cortical areas remaining approximately constant and female cortical areas declining only on an average of 10%. Principal areal moments increased with age at most cross section locations, with larger increases occuring near the tibial and femoral mid shaft and in the proximal femoral diaphysis. Changes in orientation of principal moments also occured which appear to be related to patterns of bone loss and changes in femoral neck angles with age. The study findings support the view that bone section properties reflect sex-related differences in functional loading. Changes in section properties also appear to compensate for bone loss with age so as to maintain approximately constant local stresses.

REFERENCES: Nagurka, M.L. and Hayes, W.C.: Technical note: An interactive graphics package for calculating cross-sectional properties of complex shapes. J. Biomechanics. 13:59-64, 1980.

Relationship of Isometric and Isokinetic Torques

James C. Otis, Ph.D.
Hospital for Special Surgery
Cornell Medical Center
New York, New York 10021

Isokinetic muscle testing, which measures maximal voluntary torque while the limb is constrained to move at a constant angular velocity, has become an increasingly popular method for measuring muscle performance. However, the significance of the dynamic strength measurements obtained remains unclear, particularly with respect to the relationship of isometric to isokinetic strength measurements. Osternig et al concluded that isometric strength could not be predicted from isokinetic measurements, having studied speeds ranging from 30 to 150 deg/s. The objective of this study was to examine the relationship between maximal isometric torque and maximal isokinetic torque at angular velocities of 12 and 24 deg/s for both flexion and extension of the elbow joint.

Sixteen male and 14 female subjects were tested bilaterally. A dynamometer was used to provide the constant angular velocity constraint. Torque was recorded from a strain gage torque sensor (Lebow-Model #2110H-2K) with a sensitivity of 0.15 N-m mounted on the dynamometer with its long axis coincident with the axis of the dynamometer shaft. Angular displacement was measured using an electrogoniometer. All measurements were recorded on a Gould Brush 2800 Chart Recorder. Isokinetic contractions were performed through the arc of motion between 40 and 110 degrees, and isometric contractions were performed at 60 and 90 degrees of flexion. The isokinetic and isometric contractions were alternated for the four trials and then repeated in the reverse order. Since we desire maximum efforts, only the greater value of the two trials was used in the analysis.

Linear and nonlinear regressions of isometric torque versus isokinetic torque were obtained for each muscle group at the 60 and 90 degree positions and at the 12 and 24 deg/s speeds. For the eight linear regressions performed the average correlation coefficient was $.93 \pm .04$ (Mean $\pm$ 1S.D.). However, in seven cases the intercept was greater than zero, consistent with a nonlinear frictional component being manifest. Nonlinear regressions ($y=ax^b$) resulted in a slight but significant improvement in the correlation coefficients with an average value of $.95 \pm .03$. The improved fit using the power curve demonstrated that the magnitude of the friction can be directly related to strength.

Our results have demonstrated that isometric and isokinetic torque are strongly correlated at the speeds tested. From a basic standpoint, the results demonstrate that the well established inverse relationship between force and velocity is reflected during isokinetic testing. From an evaluative standpoint, the determination of a predictable relationship between isometric and isokinetic torque can provide a useful normalized measurement parameter for evaluation of alterations in muscle performance.

Osternig et al, Arch. Phys. Med. Rehabil. 58:254-257, 1977.

"Mechanical Ratios of Selected Body Levers as they Relate to the Percent Slow Twitch/Fast Twitch Muscle Fibers Involved." by Blauer L. Bangerter, Department of Physical Education, Brigham Young University, Provo, Utah 84602.

Recent studies [1,2,3,4] show similar ratios of slow twitch (ST) to fast twitch (FT) fibres in various muscles. It was hypothesized that predominantly ST muscles would move levers in the body geared to force mechanical ratios and the predominantly FT muscles would move levers geared to speed ratios. In an effort to test this hypothesis, ST ratios of eight selected muscles [2,3] were correlated by Pearson's product moment method with the mechanical ratios of the levers these muscles move. The mechanical ratio is the quotient of Ea/Ra.* To assess mechanical ratios typical of these levers, five cadavers from the BYU Human Performance lab were carefully measured. The correlation produced an r = .860. Table 1 presents the basic data of the study. It was concluded that a high positive correlation existed between mechanical ratio of body levers and percent ST fibres of the corresponding muscles. Two examples taken from Table 1 are included for clarity. The soleus (88% ST) has a force ratio in excess of 2.6:1 and the triceps (33% ST) has a speed ratio of 10:1 or a force ratio of 0.1:1. Many muscles with their attendant levers are difficult to assess as to mechanical ratio. Also the ratio constantly changes with movement and changing angles of pull. The function a muscle is called on to perform is also variable (i.e., prime mover, stabilizer, etc.) In contrast to the data given in Table 1 (gastrocnemius 52% ST), Costill et al.[4] showed the gastronemius to average 79% ST fibres in several elite (marathon) distance runners. These men who ran 50-125 miles a week for years surely used the gastronemius in the same force ratio as the soleus. This demonstrated that the function and structure in these subjects held to an expected relationship.

Table 1

	From Cadavers (N = 5)			From Ref 2 and 3 (N = 8)	
Muscles	Mean Effort Arm-cm	Mean Resistance Arm-cm	Mechanical Ratio	Mean % ST Fibres	Range % Slow Twitch Fibres
Soleus	16.4	6.3	2.6	88	77-100
Tibialis Anterior	6.7	7.3	.92	70	58-80
Deltoid	6.4	30.6	.21	61	44-76
Biceps Br.	4.24	17.8	.24	55	37-69
Gastrocnemius-Knee	4.18	21.6	.19	52	42-64
Vastus Lateralis	4.8	21.6	.22	46	35-63
Rectus Femoris	4.8	21.6	.22	40	30-52
Triceps Br.	4.8	17.8	.10	33	17-48

*All resistance arms (RA) were measured at the center of gravity of the segment moved by the muscle and were considered at the horizontal, with angle of pull at 90^{o}, and with the effort arm (EA) the perpendicular distance from the joint to the line of muscle pull.

References

1. Saltin, Bengt; J. Henriksson, E. Nygaard, and P. Andersen. 1977. Annals New York Academy of Science. 301:3029.

2. Johnson, M.A., J. Palgar, D. Weightman and D. Appleton. 1973. Journal of Neurological Sciences. 18:111-129.

3. Nygaard, E. and T. Goricke. 1976. Report No. 99 (in Danish) August Krogh Institute, Copenhagen.

4. Costill, D.L., W.J. Fink and M.L. Pollack. 1976. Medicine and Science in Sports. 8:21 pp. 96-100.

"Strength Training: The Effects of Load and Rate of Exercise on Joint Kinetics", by James G. Hay, James G. Andrews and Christopher L. Vaughan, Biomechanics Laboratory, Department of Physical Education, University of Iowa, Iowa City, Iowa 52242.

The procedures commonly used to increase muscular strength in rehabilitation and sport are based on the simple premise that muscular tissue adapts, both structurally and functionally, in response to the stresses imposed upon it. The magnitudes of these stresses are a function of the external load and the rate at which that load is moved. The purpose of this study was to determine the effects of variations in the external load moved and the rate at which it was moved on the joint forces and torques exerted during a strength-training exercise.

Three males, experienced in the use of weight machines and barbells for strength development, were used as subjects. Each subject performed a seated arm curl under nine different conditions (3 loads x 3 rates) using a barbell and a weight-training machine. Each trial was recorded with a motion-picture camera filming at 50 frames/s and the exposed film analyzed to determine relevant kinematic and kinetic characteristics of the motion.

For all trials with the barbell, the elbow torque-time curve had the same basic form -- an initially high flexor torque; a steady decrease to an extensor torque near the completion of the lifting phase and during the initial part of the lowering phase; and a steady increase until the initial peak value was regained. The magnitudes of the torques were directly related to the load lifted. The magnitudes of the maximum values for the flexor torques (120-200 N•m) were on the order of 1.5-2.0 times those for the extensor torques.

For trials with the weight-machine the magnitudes of the maximum values of the elbow torque were markedly less than the corresponding values for the trials with the barbell. In several instances, a flexor torque was recorded throughout the entire exercise.

As the rate at which the loads were lifted was decreased, the magnitudes of the maximum torques generally decreased. The most pronounced decrease was noted when the lifting time was increased from 1 s to 2 s. The maximum torques for lifting times of 2 s and 3 s were often very similar. This supports the assumption that the system inertial effects are greatest at fast lifting speeds and decline asymptotically as the speed of lifting decreases.

The findings of this study have important implications for strength-training practices -- especially with regard to the relative merits of the barbell and weight machine -- and for the development of an understanding of the mechanicsms by which muscular tissues are stressed.

"IN VIVO" MUSCLE FORCES DURING UNRESTRAINED LOCOMOTION

Gregor, R.J. and C.L. Hager, and R.R Roy
Neuromuscular Research Laboratory, Department of Kinesiology, University of California, Los Angeles, Los Angeles, CA 90024.

While much work has been conducted on estimating skeletal muscle force production during movement by employing mathematical models or external measurements of force and acceleration, there remains a need for more direct measurements of muscle force, in vivo, during unrestrained movement. A system initially similar to that developed by Yager (3), and modified by Walmsley et al. (2) has been modified further to monitor tendon forces, in vivo, in freely moving cats. The "buckle" arrangement made of 316 stainless steel alloy, measures 16 mm in length, 7.5 mm in width and 2.5 mm in thickness. Two foil gauges (120 Ω) are applied to the top side of the element over the center of the buckle and connected to a headplug on the animal by seven strand, teflon coated stainless steel wire (304). The system is linear (.19%) to at least 6 kg and can measure forces to within 4 g of tension with no baseline drift.

In the current preparation tendon force and electrical activity (EMG) are monitored in the medial gastrocnemius (MG) and EMG in the soleus (SOL). In vivo contraction times of both SOL and MG muscles have been monitored with one buckle and two EMG implants and agree well with in situ data. Potential complications of tissue growth around the buckle as implant time progresses are compensated for in a terminal, in situ, experiment during evaluation of standard static and dynamic (F/V) properties of each muscle. Force data relative to muscle length and velocity information are evaluated according to the procedure outlined by Goslow et al. (1) but length remains an issue, especially in reference to L_0 measured in situ.

Force information from the MG muscle during standing and walking agree with values reported by Walmsley et al. (2) with electromechanical delays observed in the order of 10 msec during cat hindlimb shakes (Figure 1). Figure 2 illustrates the ability of the buckle (A), in series with an external transducer (B) (Grass FT10) to accurately respond during both twitch and tetanizing stimulations. Twitch-tetanus ratios are similar across transducers and in agreement with previous research.

(1) Goslow, G.E., Reinking, R.M. and Stuart, D.G. (1973). The Cat Step Cycle · hind limb joint angles and muscle lengths during unrestrained locomotion. J. Morphol. 141, 1-42.
(2) Walmsley, B., Hodgson, J.A. and Burke, R.E. (1978). Forces produced by medial gastrocnemius and soleus muscles during locomotion in freely moving cats. J. Neurophysiol. 41, 1203-1216.
(3) Yager, J.G. The Electromyogram as a Predictor of Muscle Mechanical Response (1972). (Doctoral Thesis), Memphis, University of Tennessee.

FIG. 1

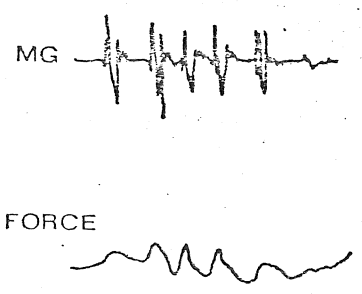

FIG. 2

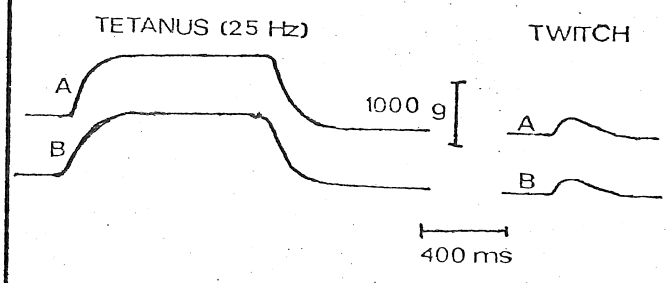

LOCAL VARIATIONS IN THE PRESSURES IN THE HUMAN HIP JOINT

T. J. Macirowski,* R. W. Mann,* and W. H. Harris+

Knowledge of the mechanical behavior of articular cartilage is crucial for analysis of the normal function of synovial joints as biological bearings and the pathogenesis of their failure in osteoarthritis.

An instrumented Moore prosthesis and a hydraulically powered and computer-controlled hip simulator was used to apply a wide range of physiological loads to the human hip in vitro and measure directly the resulting pressures. Previous work by our group has demonstrated the influence of cartilage geometry on the resulting pressure distributions (Rushfeldt 1979), and investigated the detailed geometry and congruency of human hip joints (Tepic 1980). Estimates of the maximum load across the joint while walking range as high as five or more times body weight, with significant variation in the direction of the resultant load. In this study we applied loads of approximately 2.5 times body weight (1350 N), to replicate the load vector (magnitude and orientation) occurring during the two peaks in joint load during the stance phase of gait, following heel-strike and preceding toe-off.

In the first instance, with the load directed 12 degrees medially and 8 degrees posteriorly of vertical, the maximum pressure measured within 30 sec. of the application of the load was 8.6 MN/m^2, and the average pressure of 253 spatially distributed data points was 2.3 MN/m^2. These pressures decreased to 8.0 and 2.1 MN/m^2, respectively, within 5 minutes. When the load was directed 7 degrees medially and 15 degrees anteriorly, the initial maximum pressure was 9.2 MN/m^2 with an average of 2.8 MN/m^2. After 5 minutes the average pressure decreased to 2.1 MN/m^2 as before, but the maximum pressure increased to 12.3 MN/m^2. The adverse effects of the anterior and medial loads are evident from the detailed isobar contours of the pressure distribution--more irregular pressure distribution, higher pressure gradients, and the appearance of a new and different peak in pressure anterior to that observed when the load was first applied.

This behavior illustrates two important phenomena. First, the cartilage exhibits local variation in its behavior when loaded in situ. Secondly, the behavior strongly depends on the external load conditions, even within normal physiological ranges. Together with the knowledge that the local joint geometry influences the pressure distribution, these data have important implications toward an understanding of the etiology of joint failure in osteoarthritis. Since the failure of the cartilage is typically local in scale and appears mechanical in nature, it would appear that some areas in a specific joint are more prone to failure. This work suggests that increased functional demand on localized tissue, due to variations in geometry and loading, may be important factors in the pathogenesis of osteoarthritis.

References

Rushfeldt, P. D., "Influence of Cartilage Geometry on the Pressure Distribution in the Human Hip Joint," Science, 204, 413 (1979).

Tepic, S., "Congruency of the Human Hip Joint," S. M. Thesis, M.I.T. (1980).

Supported by the Whitaker Professorship of Biomedical Engineering, M.I.T. and NIH Grant AM16116.

---

*Mass. Institute of Technology, 77 Mass. Ave., Rm. 3-147, Cambridge, MA 02139

+Mass. General Hospital, Orthopaedic Research Laboratory, Boston, MA

QUANTITATIVE SYNOVIAL JOINT GEOMETRY AND LOAD DISTRIBUTION

R. W. Mann,* P. D. Rushfeldt,* and W. H. Harris+

Although vertebrate synovial joints serve as mechanical bearings between articulating body segments, detailed quantitative experimental data on how interarticular forces are distributed as pressure across the juxtaposed cartilage layers and how in turn the thin cartilage layers deform, both globally and locally, have been virtually unavailable. Now for the human hip joint, pressure distribution and cartilage geometry are measured in vitro in an integrated hip simulator/computer facility.

The global morphology and localized geometry of both acetabular and femoral components are established by an ultrasonic technique. Reflections from the unloaded interarticular surface and from the calcified cartilage-subchondral bone interface permit calculation of these distances from the center of a spherical coordinate system, for three hundred discrete locations on the femoral head and one hundred fifty on the acetabulum. A computer program determines the least-square, best-fitting spheres for each of the four surfaces and plots conic projection contour maps of local elevations and depressions and isothickness maps of cartilage thickness distribution.

Pressure distribution across the acetabulum interarticular surface is measured in the hip simulator using a pseudofemoral head prosthesis, the load-bearing spherical surface of which includes fourteen pressure transducers. Computer programs control prosthesis/acetabula force and movement and produce isobar contour maps of pressure distribution. Load magnitude, hip flexion/extension, abduction/adduction, and internal/external rotation angles can be controlled statically or dynamically, separately or in synchrony, thereby simulating most aspects of in vivo hip-joint loading/motion. Thus the pressure distributions can be produced at different times following initial loading, for different loads, along different load axes, for different quality of "fit" between prosthesis and acetabulum, etc. The consolidation of cartilage is measured to several μm accuracy along the load axis; the relative position of the loading sphere in the acetabulum is established by a concurrent ultrasonic measurement.

Geometric measurements show that (1) unloaded cartilage surfaces of both femoral head and acetabula are spherical with local deviations generally within 100 μm, reaching 200 μm only in very small perifoveal or peripheral regions of the femoral head; (2) maximum deviations from sphericity at the calcified cartilage interface are of the order of 500 μm; (3) the centers of the calcified interface best-fitting spheres are shifted with respect to the centers of the surface best-fitting spheres resulting in increased average cartilage thickness at the superior anterior medial aspect on the femoral head and decreased thickness at the same aspect of the acetabulum.

The corresponding pressure distributions vary with time after loading, are highly irregular--elongated in the anterior-posterior direction with pressure ridges and valleys frequently displaying multiple maxima--and exhibit local pressure far in excess of that previously estimated.

Similarities in the shapes of the pressure isocontours and the percent cartilage compression isocontours under the same loading conditions suggest that geometric aberrations in the cartilage layer strongly influence pressure distribution, particularly irregularities at the calcified cartilage-sub-chondral bone interface, which appear to produce the most intense pressures and pressure gradients.

Supported by the Whitaker Professorship of Biomedical Engineering, M.I.T. and NIH Grant AM16116

*Mass. Institute of Technology, 77 Mass. Ave., Rm. 3-144, Cambridge, MA 02139

ANALYTICAL MACROGEOMETRY REPRESENTATION AND CONGRUENCY OF THE HUMAN HIP JOINT

S. Tepic,* R. W. Mann,* and W. H. Harris+

The global geometry of the movable joint, particularly of the articulating surfaces, is essential to its function. Three aspects of the joint geometry (a) the articulating surface shape; (b) cartilage thickness distribution; and (c) interarticular congruency of joint components have been treated as separate issues in most of the literature. Our in vitro ultrasonic technique, described in detail elsewhere, [1], [2], [3], and the analytical treatment outlined here, provide an integrated, well-defined and systematic approach to geometrical investigations of the human hip joint.

Cartilage-bounding surfaces of both joint components are measured separately in the spherical coordinate systems of the corresponding scanners at a set of points (θ_j, ϕ_k) given by: (i) roots θ_j of the Legendre polynomial of degree 20, and (ii) $\phi_k = k\pi/20$, $k = 0, 1, 2 \ldots, 39$. The data are organized in four 20 x 40 matrices $R = [r_{jk}]$. For the purpose of shape description alone, the matrix R will suffice; sphericity studies via least-square-fitting to discrete points, [2], [4], permits a concise, well-organized data presentation. However, issues such as congruency, where the shapes of two opposing surfaces are to be compared, require some form of analytical representation.

Spherical harmonics Y_{lm} were chosen as the base to form $r(\theta,\phi) = \Sigma\Sigma\, A_{lm}Y_{lm}$ globally fitted to the r_{jk}'s of the matrix R. In evaluating coefficients $A_{lm} = \int_{\Lambda} r \cdot Y^{*}_{lm}\, d\Omega$ the Gauss-Legendre formula was used for integration over θ (the reason for the particular choice of scanning locations) and trigonometric interpolation was used over ϕ. The cartilage covered area offers about three hundred measurement locations on the femoral head and about one hundred fifty in the acetabulum--only a portion of eight hundred elements in R matrices. The missing elements are generated through an iterative procedure which was found to increase the rate of convergence over the true data sufficiently to allow approximation within experimental error when 19th degree harmonics are used.

As reported in [1] and [4] the unloaded articulating surfaces of the hip joint are spherical to within 200 μm, but questions remain on how minute deviations from sphericity of the opposing sides relate in articulation. The analytical representations of the surfaces in combination with a congruency parameter provide clear problem formulation and permit particular solutions.

Given two surfaces, S_1 by r_1 on Ω_1, and S_2 by r_2 on Ω_2, $\Omega_1 \cap \Omega_2 \neq [0]$, define a congruency index as:

$$\zeta(S_1,S_2) = \left[\int_{\Omega_1\cap\Omega_2} (r_1 - r_2)^2 d\Omega\right]^{-1} \int_{\Omega_1\cap\Omega_2} d\Omega\,,$$

and consider $r \circ t$: $S_2 \rightarrow S_2' \mid r \circ t \in \mathcal{R}x\mathcal{T}$, where $\mathcal{R}$ and $\mathcal{T}$ are sets of allowed rotations and translations of S_2 in R^3. (Translations occur as the mating components under compressive load seek the lowest energy relationship.) We are interested in properties of $F: \mathcal{R}x\mathcal{T} \rightarrow \zeta(S_1,S_2)$, particularly its extrema, when S_1 and S_2 represent articulating surfaces of the acetabulum and the femoral head, respectively.

For hip angular positions typical of one-legged stance over the physiological range of flexion-extension angle σ, ζ was maximized with respect to small translations. The resulting congruency curve $\zeta_{max|t}$ vs. σ exhibits prominent extrema whose locations suggest possible causal relationships between joint function and joint congruency.

References: 1. Rushfeldt, P. D., Mann, R. W. and Harris, W. H., Science, 204:413, 1979.
2. Rushfeldt, P. D., Sc.D., Thesis, M.I.T., 1978.
3. Tepic, S., Mann, R. W., and Harris, W. H., 26th Ann. ORS Mtg., 1980.
4. Tepic, S., S. M. Thesis, M.I.T., 1980

Supported by the Whitaker Professorship of Biomedical Engineering, M.I.T. and NIH Grant AM16116.

*Mass. Institute of Technology, 77 Mass. Ave., Rm. 3-147, Cambridge, MA 02139
+Mass. General Hospital, Orthopaedic Research Laboratory, Boston, MA

2.R
3,4

A NEW FEMORAL LOADING RIG

By - P. S. Walker, Ph.D., M. Ben-Dov, M.S.; and A. J. C. Lee, Ph.D.* -
Howmedica, Inc., 359 Veterans Boulevard, Rutherford, N.J. 07070
* Permanent address - University of Exeter, U.K.

The clinical performance and biological reaction to hip prostheses, nails, etc., in the upper femur depend on the load transfer between the device and the bone, and on the stress states at multiple locations in the bone. For examples the osteopaenia seen in the calcar area may be a result of grossly non-physiological stresses. Loosening at the implant-bone interface may likewise be a result of the stresses transferred at the interface.

Most of the literature reports have treated the frontal plane only. However, the forces and moments in the sagittal plane could be of great significance, and the effects are in need of investigation.

Our objective was to construct a rig for loading the femur, with the following specifications:

1 The lower end of the femur fixed to resist forces and moments.

2 Loads applied to the femoral head and to the greater trochanter by a lever mechanism simulating the pelvis and the body in a one-legged stance.

3 The femoral head free to move vertically and horizontally in response to the loads.

4 Variability of angulation of the axis of the femur, in the frontal plane and in the sagittal plane.

5 Automatic control and monitoring of applied load and angles, the abductor force, and the femoral head force.

6 Monitoring and digital print-out of the strains at points on the femur and on any implanted device.

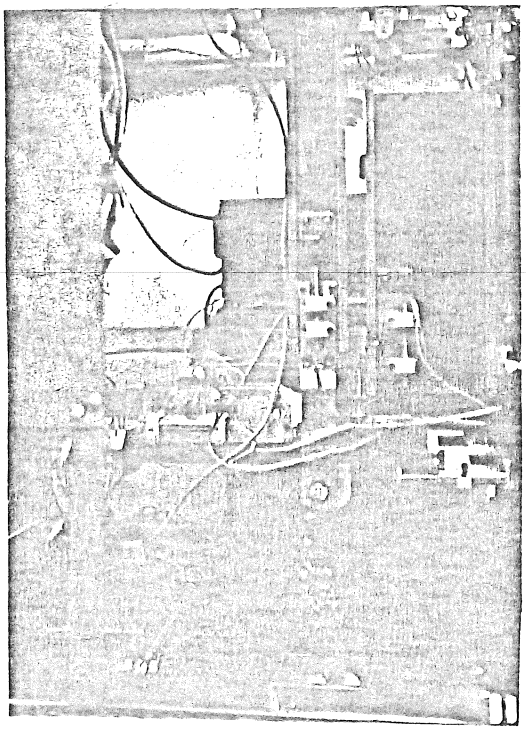

Both the body load and abductor force can be varied in size and location. The frontal and sagittal angles are controlled with DC motor driven electric cylinders. The level of the arm is continuously controlled by LVDT feedback. All of the required angles and loads are pre-programmed, and all of the angular, linear, and force data are stored and then displayed on an HP system. Early results on femurs show the versatility and ease of operation of our system.

References:

Oh & Harris, JBJS, 60-A:75, 1978.

Crowninshield, Brand & Johnson: Proc. Orthop. Res. Soc., San Francisco, 1979.

Acknowledgements:

We acknowledge the contributions of T. Helder, L. Ferus, A. Enayati, and A. LeRoy.

A Strain Energy Function For A Guinea Pig Gallbladder

by
N.Guzelsu,Ph.D.,L.S.U.M.C. Dept.of Orthopaedics, Box 33932,Shreveport,LA,71130

Mechanical properties of a soft biological tissue in its passive state can be characterized by a proper strain energy function.The experiments run by Fung et.al,(1) on rabbit arteries , implied that an exponential type strain energy function is a better representing model than a polynomial type.

Here an exponential type strain energy funtion is used for determining the passive elastic response of the gallbladder.It is assumed that, a guinea pig gallbladder is incompressible, homogeneous and isotropic. Incompressibility is accepted widely for soft biological tissues(2).For the gallbladder,the other assumptions are supported by the simple tension experiments of the gallbladder rings of different positions and orientation which are obtained by cutting intact gallbladders(3).Under the above assumptions, a general exponential type strain energy function (Σ) which contains three physical constants(α, β, γ) can be written in the following way.

$$\Sigma = \alpha \left(\exp \{ \beta (I - 3) + \gamma (II - 3) \} - 1 \right) \qquad (1)$$

Where I and II are the first and the second strain invariants, respectively. The relation between the applied load (N) and the streches (λ) of the gallbladder ring which has a a uniform initial cross section (2A) is given,

$$N = (2\alpha)(2A)\left(\lambda\beta - \beta/\lambda^2 + \gamma - \gamma/\lambda^3 \right) \exp\{ \beta(\lambda^2 + 2/\lambda - 3) + \gamma(2\lambda + 1/\lambda^2 - 3) \} \qquad (2)$$

The experimental points of applied load N versus stretch λ of the gallbladder rings are shown in Figure 1. Figure 2 shows the experimental points in a semi-logarithmic scale. Examination of figure 2 suggests that an exponential type curve ($N = c_1 \exp \{ c_2 \lambda \}$, c_1 and c_2 are constants) can be fitted to the experimental points by using the method of least squares. The comparison of the fitted curve with the equation (2) suggests that the strain energy function (1) with two physical constants α , γ ($\beta = 0$) can describe the mechanical behaviour of the guinea pig gallbladder with a good accuracy. The theoretical curve for $\beta = 0$ is shown in figure 1 and 2 .(α=117.6N/m^2,γ= 0.84).

An experimental curve, in a semi-logarithmic scale, (N or stress versus λ) of a simple tension or other type simple loadings can give enough information in choosing the simplest energy function for biological tissues.

1-Fung,Y.C.,K.Fronek and P.Patitucci(1979)Biomechanics Symposium AMD-Vol 32 The Am. Soc. Mech. Eng. pp.115
2-Carew,T.E. (1968) Circulation Research Vol.23 , pp.61.
3-Guzelsu,N., and P.Biancani(1980)Submitted to the American J. Physiology

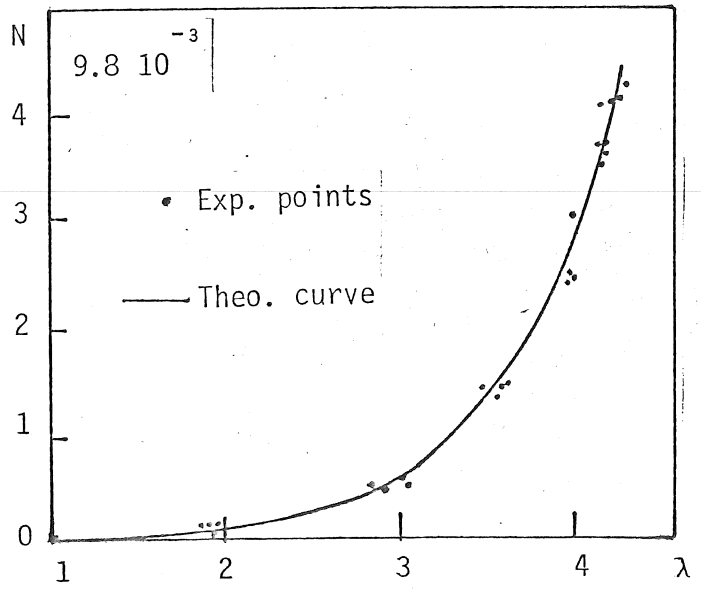

Figure 1

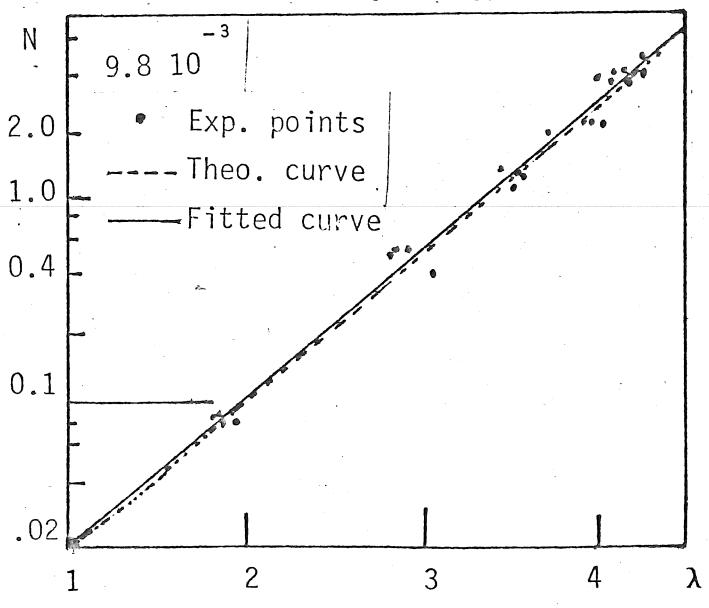

Figure 2

AN ANALYSIS OF SOFT TISSUE LOADING IN THE FOOT

Roy D. Crowninshield, Ph.D.
Sachio Nakamura

Biomechanics Laboratory
Department of Orthopaedic Surgery
University of Iowa
Iowa City, Iowa

During the performance of everyday activity, the foot is subjected to repeated loading which, in many cases, represents constant trauma and misuse. The biomechanical behavior of the foot is, at present, not well understood. In particular, the magnitudes of stresses developed within the plantar skin during foot function and the dependency of these magnitudes on shoe design is not well known. Knowledge of this stress has application in both medicine and sports. Excessively high stresses on the foot can cause dermatological complications that are particularly important to diabetics. These patients have an unfortunately high incidence of lower extremity amputation as the result of foot skin breakdown. The sports enthusiast, in particular distance runners, may also benefit from an improved understanding of shoe designs role in stress development within the foot.

This presentation reports on a planar, large displacement and nonlinear finite element stress analysis of the foot within a shoe. The foot is modeled with a bony skeleton and plantar region of thick skin. An experimental determination of skin material properties revealed a highly nonlinear and nearly incompressible behavior. The elastic properties of the shoe sole is represented in the model by a variety of both linear and nonlinear materials. Shoe soles were considered with regards to their effect on the resulting stress developed within the plantar skin.

The results indicate a significant dependency of the maximum stress within the foot on the elastic properties of the shoe sole. The figure below demonstrates a typical result of maximum compressive stress within the foot during mid-stance for a variety of shoe sole moduli of elasticity. Experimental measurement of foot surface pressure is ongoing and may be employed as a validation of this analytical prediction.

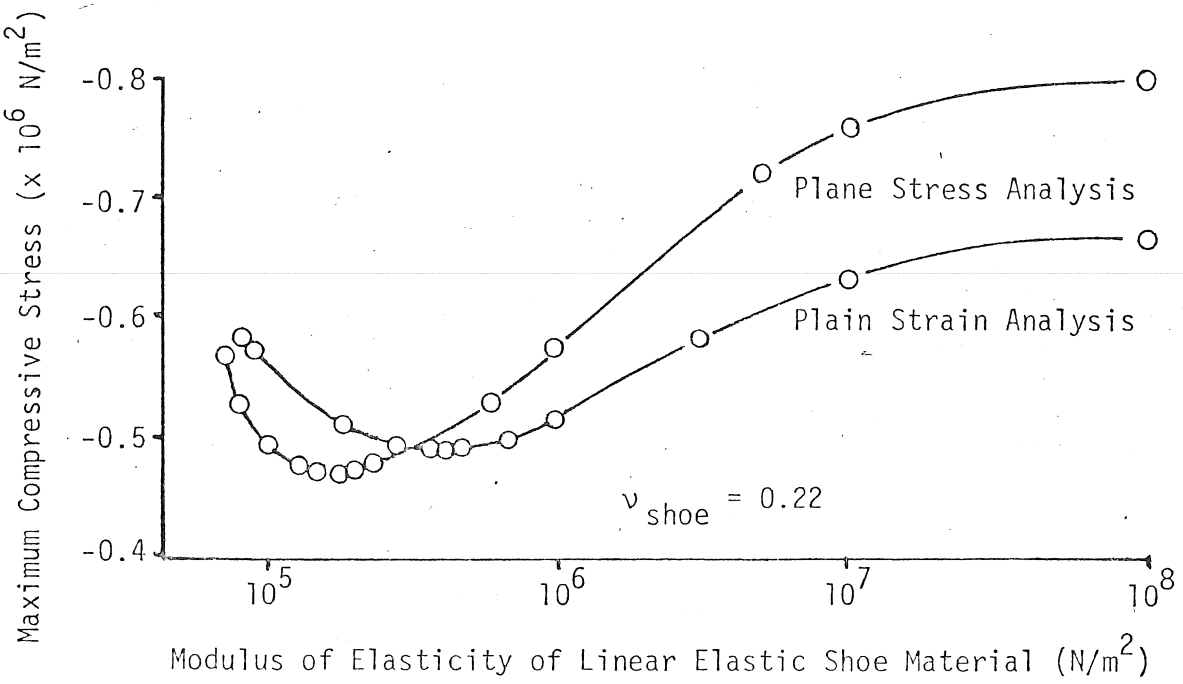

ENHANCED DIFFUSION IN LUNG GAS MIXING

H.D. Van Liew and D.J. Wilkinson
Department of Physiology
State University of New York at Buffalo
Buffalo, New York 14214

It has recently been reported that life can be maintained without breathing; when an oscillating current (15 Hertz) of gas is directed into the trachea of an anesthetized dog, there is very little change of lung volume with time but O_2 and CO_2 exchanges are normal (1). A suggested explanation is that small convective movements facilitate molecular diffusion of gas. It has been suggested that a similar facilitation may occur in ordinary breathing because of convective disturbances caused by the heart beat (2).

To shed light on these matters, we attempted to match experimental data with simulations done by computer. Our computer model combines diffusion equations with morphometric equations to provide simulations of molecular diffusion in a lung-shaped vessel. Because mixing in the lung is ordinarily so effective that there is little to observe, we used experimental data from men breathing in a hyperbaric chamber; in a high pressure environment, mixing is markedly poorer than normal (3).

When we used molecular diffusivity values and the recorded breath time as inputs to the model, the predicted amounts of gas to exchange between inspirate and residual lung gas were far less than measured amounts. However, when inputs for either diffusivity or time allotted for diffusion where increased, predictions corresponded to measurements surprisingly well, both in amounts exchanged and in pattern of concentration vs volume expired. We found the enhancement factor to be about 6.0; essentially the same value was estimated by Fukuchi *et al.* (2) from measurements made inside small lung airways by a completely different approach. Apparently in normal breathing the coefficient of "effective diffusivity" in the lung is about 6 times larger than the coefficient of molecular diffusivity.

1. Bohn, D.J., K. Miyasaka, B.E. Marchak, W.K. Thompson, A.B. Froese and A.C. Bryan. Ventilation by high-frequency oscillation. *J. Appl. Physiol.* 48: 710-716, 1980.

2. Fukuchi, Y., C.S. Roussos, P.T. Macklem and L.A. Engel. Convection, diffusion and cardiogenic mixing of inspired gas in the lung: an experimental approach. *Respir. Physiol.* 26: 77-90, 1976.

3. Van Liew, H.D., E.D. Thalmann and D.K. Sponholtz. Diffusion-dependence of pulmonary gas mixing at 5.5 and 9.5 ATA. *Undersea Biomed. Res.* 6: 251-258, 1979.

(Supported in part by NHLBI Grant PO1-HL-14414 and ONR Contract N00014-76-000472.)

MASS TRANSPORT TO PULSATILE FLOWS IN CIRCULAR TUBES GIVEN CURVATURE IN VARIOUS DIFFERENT PATTERNS

P. D. RICHARDSON, P. M. GALLETTI and K. TANISHITA
Brown University, Providence, R. I. and Tokyo Women's Medical College, Tokyo

Implantable artificial organs, including lungs, hybrid pancreas and liver, can benefit from high mass transport rates at their wall surfaces. Blood flow through such devices is inherently pulsatile when driven by the natural heart. It has been known for some time[1] that curvature of the tube induces secondary motions and that with these the mass transport rates are enhanced, especially for the high Schmidt-number situations typical of the biomedical applications. Recent analyses[2,3,4] have concentrated on flow and transport in helically-coiled tubes, but curvature can be given to tubes conveniently in various other different patterns, and it is quicker to evaluate the relative merits of such different patterns by experiment then by extension of the analysis.

A series of curved-tube devices was fabricated with various different patterns of curvature. These included helical coils, serpentines, S-shaped forward-and-reversed spirals and woven (macramé) shapes. The tubing used was microfibrillar Teflon, a hydrophobic material which can be wound with high curvature (small radius of curvature) without kinking. An apparatus was constructed for carrying out mass transport experiments in vitro. This consisted of a motor-driven syringe pump capable of providing steady flows up to 3L/min, coupled with a variable amplitude, variable frequency pulsator pump which produces simple harmonic motion by a motor-driven scotch yoke mechanism. All parts were made sufficiently rigid that pulsation did not interfere with the steadiness of flow obtained from the syringe pump. Transport of O_2 and CO_2 was measured over a wide range of water flow rates through the curved tube devices, and over a range of about 10:1 in pulsation frequency and amplitude. Some transport measurements were also made using sheep blood.

Over the ranges of Dean number and Womersley number covered it was found that the mass transfer coefficients correlated best with the characteristic pulsation velocity, that in highly pulsatile flow the mass transfer coefficients were independent of the mean flow rate, and that the patterns of curvature were less important than curvature itself in causing augmentation of transport: repeated reversals of curvature, as in a woven pattern, do not cancel out the benefits of curvature.

References

1. W. R. Dean, Phil. Mag. Series 7, 4, 208, 1927.
2. W. H. Lyne, Jl. Fluid Mech. 45, 13, 1971.
3. F. T. Smith, Jl.Fluid Mech. 71, 15, 1975.
4. P. J. Blennerhassett, Ph.D. thesis, U. of London, 1978.

ALTERED STRESS FIELDS CREATED BY THE APPLICATION OF DIFFERENT FRACTURE PLATES TO THE CANINE FEMUR

D.R. Carter, R. Vasu, and W.H. Harris (Orthopaedic Research Laboratories, Massachusetts General Hospital and Harvard Medical School, Boston, MA 02114).

The application of a plate to a long bone which has been fractured can establish excellent bone alignment. After the fracture has healed, however, the plate transmits a portion of the loads which are normally transmitted by the bone. Significant bone remodeling and a net bone loss may occur which many researchers attribute to the changes in in vivo bone stresses. Experimental studies by Akeson et al. (1975), Tonino et al. (1976), Moyen et al. (1976) and Bradley et al. (1979) indicate that, in general, greater bone remodeling and bone loss is observed when stiff plates are used than when more flexible plates are used. In the present study, we used the in vivo strain gage results reported by Vasu et al. (1980) to estimate the in vivo stress fields in the normal canine femur during the mid-stance phase of the gait cycle. Determinations were then made of stresses due to the application of the various plates used in the previous studies mentioned. The results of the previous plating experiments were then interpreted in light of the altered in vivo stress fields as calculated in this investigation.

To investigate the influence of plating on the cyclic bone stress fields in these animals, we cut a mid-femoral cross section from a 21 kg dog. This section was photographed and enlarged. The enlarged section was divided into 80 discrete elements and the area and moments of inertia were determined. We assumed that the cyclic stress fields imposed on this section were similar to those measured on the section from the 35 kg dog. That is, 1) during the swing phase the intracortical stress fields were negligible, and 2) during the stance phase the stresses were -5.1 MPa postero-medially, 2.3 MPa antero-laterally, and 0.0 MPa laterally. We then calculated the resultant axial force and bending moments during gait. During the swing phase, these resultants were negligible since no significant bone stresses were created. To calculate P, M_x, M_y during the stance phase, we employed the combined flexural formula. To determine the intracortical stress fields during the stance phase the calculated load resultants were substituted back into the flexural formula to solve for stresses at any (x,y) location.

The influence of plate attachment on the bone stress fields was determined using composite beam theory. This analysis was done for ten different plating configurations used in bone metabolic studies by other researchers. Our calculations suggest that the canine femur is very sensitive to what may appear to be small changes in in vivo cyclic stress. In the study by Akeson et al. as well as that by Moyen et al. very significant differences in bone remodeling were shown after plating with two different plate types. The differences in local bone cyclic stresses in the plates studied, however, was in the range of one MPa. This finding is quite striking if one considers that this change in cyclic stress is approximately one percent of the ultimate strength of the bone tissue.

Vasu et al. (1980) Proc. 8th N. E. Bioengineering Conference 8:425-428.
Akeson et al. (1975) Calcif. Tissue Res. 19:27-37.
Tonino et al. (1976) J. Bone Joint Surg., 58B:107-113.
Moyen et al. (1978) J. Bone Joint Surg., 60A:940-947.
Bradley et al. (1979) J. Bone Joint Surg., 61A:866-872.

Supported by NIH grant AM 27117

EXPERIMENTAL EXTERNAL FIXATION

Scott Stanwyck
M. H. Pope
David Seligson

An external fixation device is a mechanical substitute for the skeleton made by placing pins in bone and joining the pins together in a frame. Studies by Whie, Panjabi, Southwick, in rabbits have showed that there are phases of fracture healing under external skeletal fixation. Two basic mechanisms for fractured healing have been proposed, one in which the bone repairs itself directly - primary bone union, and the second which healing takes place through a cartilagines phase - the callous. The present experiment was conducted in a large animal, the sheep, to determine the bio-mechanics of fracture healing under external fixation.

A simple external fixateur was fabricated for placement on the tibia of a sheep. The plan was to place a fixateur on both limbs to try to achieve a fracture held in an anatomical position and to load one of the fixateurs so there would be compression at the oteotomy. With bilateral fixation the animal used the compressed limb more than the uncompressed limb, and therefore the experiment did not provide a similiar mechanical environment for both fractures. Then an experiment was done with four sheep, two limbs loaded and two limbs not loaded. As expected during the healing of the fracture the animals with the compressed fractures were more stable on their legs and used them sooner. Sheep were all ambulatory by two weeks. At eight weeks the sheep were X-rayed, sacrificed, and mechanical testing and histologic examination performed on the fracture specimens. This data is collected in Table I.

Animal	Compression	4-Point Bending (Nt. m/m x 10^3)	X-rays	Histology
WO	0	1.0	1mm distraction	Secondary healing callus
WA	Yes	0.8	4mm off-set	Secondary healing callus
M	Yes	1.0	2mm off-set	Secondary healing callus
H	0	0.4	Delayed Union	Inflammation

Table I. Biological and mechanical paraments of eight week healed sheep tibae fracture treated with external fixation.

Ref. White, Panjabi, Southwick: The Four Biomechanical Stages of Fracture Repair, J Bone Joint Surg 59A:188-192, 1977.

This work sponsored by a grant from the Whitaker Foundation.

TORSIONAL STRENGTH OF HEALING FRACTURES VS. OSTEOTOMIES

R.B.Martin and Charles M. Davis
Orthopedic Research Laboratories
Dept. of Orthopedic Surgery
West Virginia University, Morgantown, WV 26506

INTRODUCTION

Most studies of fracture healing in animals have actually utilized an osteotomy as the "fracture" in order to standardize the lesion to be healed. Those studies in which the bone was actually broken in bending have not included any investigation of the mechanical properties of the healing callus. We have developed a method for producing closed fractures in the rabbit tibia using 3-point bending and for mechanically testing the callus in torsion after a given healing time. In comparative studies we have found significant differences between healing osteotomies and "true" or closed fracture.

METHODS

Male white New Zealand rabbits (2.7 - 3.2 kg) were anesthetised with halothane. Closed fractures were produced by 3-point bending of the left tibia using a special jig in a hydraulic materials testing machine. The fracture was made slightly proximal to the tibio-fibular junction using a deformation rate of about 0.1 cm/sec; a load-deformation curve was recorded during the fracture process. The fresh fracture was assessed for stability, x-rayed and the entire leg was cast in waterproof plaster. Osteotomies were handled in similar fashion except that the proximal tibia was exposed and severed with a Gigli saw. Five weeks post fracture, the healing bones were x-rayed, assessed for stability, weighed, tested to failure in quasistatic torsion, and demineralized for H&E and Safranin O sections. Angulation, displacement and amount of mineralized callus were measured from the terminal x-rays.

RESULTS

See Table 1. It was found that the fractures and osteotomies were similar in terms of bone mass, amount of callus, and degree of angulation, but the latter group exhibited less displacement, perhaps because transverse saw cuts do not override as easily as oblique fracture surfaces. More importantly, the 5 week callus was significantly weaker (P=.03) in the case of osteotomies. This observation has obvious implications in terms of post operative management of osteotomies. It also indicates that using osteotomies as models for fracture healing may lead to important misrepresentations of the strength of a healing fracture. Currently we are investigating the reasons for these differences.

TABLE 1

Test Group	No. Rabbits	Ant. Callus*	Displ.*	Tor. Str., N-M
3 pt. bending fx.	15	2.5±.5	2.2±1.2	2.91±.88
Osteotomy	6	2.2±.4	1.0±1.1	1.95±1.14

* scale of 1 (small) to 3 (large)

Quantitative Anatomical Comparison of Human, Baboon, Dog and Sheep Femora Suitability for Implant Fixation Studies

Strongwater, A.R., Goel, V.K., Panjabi, M.M., Drinker, H.

The problem of mechanical loosening and subsequent failure of implant fixation represents the most significant threat to the further development of joint implant surgery. There are many factors responsible, but the main determinant seems to be the biomechanical changes at the bone cement interface over time. It is essential to study the interface through a suitable animal model. The demands for such a model are several: 1) femoral anatomy, joint load vectors and femoral blood supply similar to the human; 2) femoral size appropriate to reproducable total hip reconstruction techniques similar to those used in human practice; 3) a nonsedentary animal which will exercise enough to stress the implant, is docile enough to handle, and available for purchase and maintenance at a reasonable cost. No true bipedal primates are available for laboratory use. Alternatively the choice of a quadruped raises the question of whether a primate, carnivore or artiodactyle best fulfills these criteria. The purpose of the present study was to quantitate differences in the femoral anatomy of the human, baboon, sheep and dog.

Ten adult femora from each of the above species were obtained. To study external anatomy the bones were photographed in the coronal and transverse planes. To study cancellous bone distribution each specimen was then serially sliced into sections and photographed. The parameters studied were obtained by digitizing each of the paired photographs. Similarly, the distribution of cancellous bone was quantitated by determining its cross-sectional area as a function of length.

The data obtained was non-dimensionalized with regard to the length between centers of femoral head and intercondylar notch. A number of parameters like neck shaft angle, head and neck diameters, anteversion angle, etc. were compared. The parameters studied reveal that, on the whole, the external femoral anatomy of the dog is more similar to the human than the other species. The major portion of the proximal cancellous bone is located in the greater trochanter, neck and head regions. Its most distal extent for the species studied was observed in the human, followed by progressively less medullary cancellous bone in the baboon, dog and sheep.

The external parameters investigated collectively suggest that the greatest similarity to be between the dog and human. The internal parameters studied revealed a similarity between the baboon and human. Based on anatomical criteria, of the species studied, either the dog or baboon would appear a reasonable model. Additional considerations such as, cost of procurement, availability and ease of handling make the dog a more practical choice. In addition, the baboon is a sedentary animal and difficult to exercise. Therefore, of the species included in the present study, the dog would appear to be the most appropriate model for the study of femoral implant fixation. Additional comparative studies are planned to study joint kinematics and femoral blood supply to verify this choice.

Work supported in part by R.R.A.G., Veterans Administration and Yale University Grants.

Adress: Section of Orthopaedic Surgery, Yale Medical School, New Haven, CT 06510.

ON PARACHUTIST DYNAMICS

Ronald L. Huston*
and
James W. Kamman
University of Cincinnati
Cincinnati, Ohio 45221

ABSTRACT

The dynamics of a parachutist is discussed and the results of a computer simulation and a parameter study are presented. A variety of initial parachutist configurations prior to "opening shock", are considered and the relative effects on the parachutist's dynamics - particularly, the head/neck system dynamics - are studied. The objective of this parameter study is to determine those initial configurations which will minimize the force and moment pulses experienced by the head/neck system during the parachute opening.

The simulation is based upon a three-dimensional, gross-motion, finite-segment model of the parachutist. This model is developed from a modification and specialization of the UCIN Crash Victim Simulation Code (References [1] and [2]). It consists of 13 linked bodies representing the parachutist's torso, limbs, head, and neck. Nonlinear springs and dampers are used to model the joint moments. The applied forces on the model consist of riser forces from the parachute and wind forces. The riser forces, applied to the torso, are obtained from data recorded from physical jumps. The wind loading is modelled as a profile drag on each body of the model.

The modelling and simulation uses Lagrange's form of d'Alembert's principle (Reference [3]) to obtain the governing dynamical equations of motion. This principle incorporates the advantages of Lagrange's equation (for example, automatic elimination of non-working internal constraint forces), but it avoids the corresponding disadvantages (that is, differentiation of lengthy scalar energy functions) particularly when applied with multibody systems such as a parachutist model. The model also uses relative orientation angles (as opposed to absolute orientation angles) to define the parachutist's configuration. (This is to facilitate data input and data output interpretation.) The governing differential equations are solved numerically using a Runge-Kutta technique.

The results of the simulation and the parameter study are used to identify optimal initial (pre-opening) configurations. The application in parachute design, and in the development of jumping strategies, are discussed.

References

1. Huston, R. L., Hessel, R. E., and Winget, J. M., "Dynamics of a Crash Victim - A Finite Segment Model", AIAA Journal, Vol. 14, No. 2., 1976, pp. 173-178.

2. Huston, R. L., and Passerello, C. E., "On Multi-Rigid-Body Systems Dynamics", Computers and Structures, Vol. 10., 1979, pp. 439-446.

3. Huston, R. L., and Passerello, C. E., "On Lagrange's Form of d'Alembert's Principle", The Matrix and Tensor Quarterly, Vol. 23., No. 3., 1973, pp. 109-112.

*Correspondant: Mail Location No. 163 Telephone: 513/475-6131

RESPONSE OF A SIMPLIFIED INTERVERTEBRAL DISC MODEL UNDER COMPLEX LOADING; R.L. Spilker and D.M. Daugirda; Department of Materials Engineering, University of Illinois at Chicago Circle; Chicago, Illinois 60680.

A simplified axisymmetric finite-element model of the vertebral body-intervertebral disc is described which employs three homogeneous substructures corresponding to the vertebral body/endplate region, the annulus fibrosis of the intervertebral disc, and the nucleus pulposis. The first two regions are modeled as istropic materials with the vertebral body/endplate region treated as nearly rigid compared with the annulus. The nucleus is modeled as an incompressible, inviscid fluid. The response of the model to compression, torsional, shear, and moment loadings is examined. A Fourier series representation of circumferential behavior allows the analysis to be reduced to a two-dimensional model for each loading case.

The model is used to examine the effects of gross disc geometry and material property parameters on predicted intradiscal pressure increase, disc bulge, and other pertinent displacement quantities. The results obtained indicate that all parameters have a significant effect on disc displacements. Only compressive loading produces increases in intradiscal pressure, and these pressure increases are most strongly affected by changes in disc height and radius. For torsional and moment loading, predicted displacements are shown to correlate reasonably with strength of materials solutions. Results obtained with this simplified model are also shown to be in reasonable agreement with published experimental measurements, with appropriate choice of material property parameters.

MASS DENSITY DISTRIBUTION ALONG THE BODY AXIS*

H.K. Huang , Peter Weiss, D.D. Robertson, F.R. Suarez
Department of Physiology & Biophysics, Georgetown University Medical School
Washington, D.C. 20007

We have reported on the methodology of a non-destructive method for evaluating the body geometry and its physical properties based on computerized tomographic (CT) scans (1). The purpose of the paper is to present some of the data obtained from this method.

Five cadaveric specimens, ranging in age from a newborn infant to a seven year old child, have been studied using this method. Each specimen was scanned from the head to the ankle joints at 1 cm increments. Each CT scan produces a cross-sectional image of the body cross section under consideration. The CT image can then be related to the mass density distribution of the scanned section. Using standard picture processing techniques and formulas for discrete masses in mechanics, the mass, area, specific gravity, geometrical center, center of gravity, and intertia tensor for each cross section are estimated.

For each parameter, the sectional quantity versus the body axis can be plotted, demonstrating the distribution of the parameter along the body. Figures 1 and 2 are examples which show the mass and the specific gravity distributions along the body axis of a three year old specimen. It can be seen from the mass distribution plot that the head, shoulders, mid-abdomen, hip joints, knee joints and ankle joints are the local maxima, whereas the neck, lower chest, lower abdomen, lower thighs, and lower legs are the minima. From the specific gravity distribution plot, it can be seen that the head and the legs have specific gravities greater than one, whereas the torso values are less than one, except at the shoulders and hip joints. This is due to the fact that the head, legs, and joints consist of more bone than the other parts of the body. From inertia tensor distribution plots, we see that I_{xx} (x: medial-lateral) has a higher value in the head, I_{yy} (y: anterior-posterior) has a higher value in the chest, and I_{zz} (z: superior-inferior) has a higher value in both the head and chest, thus reflecting the geometry of the body structure.

Some immediate applications of this data are use as input to lumped parameter biodynamic models, in computer simulation of vehicle crash victims, and in the design of car crash dummies.

(1) H.K. Huang, et. al. "Utilization of CT Scans as Input to Finite Elements Analysis," Proc. Intern. Finite Elements in Biomechanics, Feb. 18-20, 1980, pp. 797-816.

* This research is supported by NHTSA, Department of Transportation (Contract No. DOT-HS-7-01661).

Figure 1

THREE YEAR FEMALE

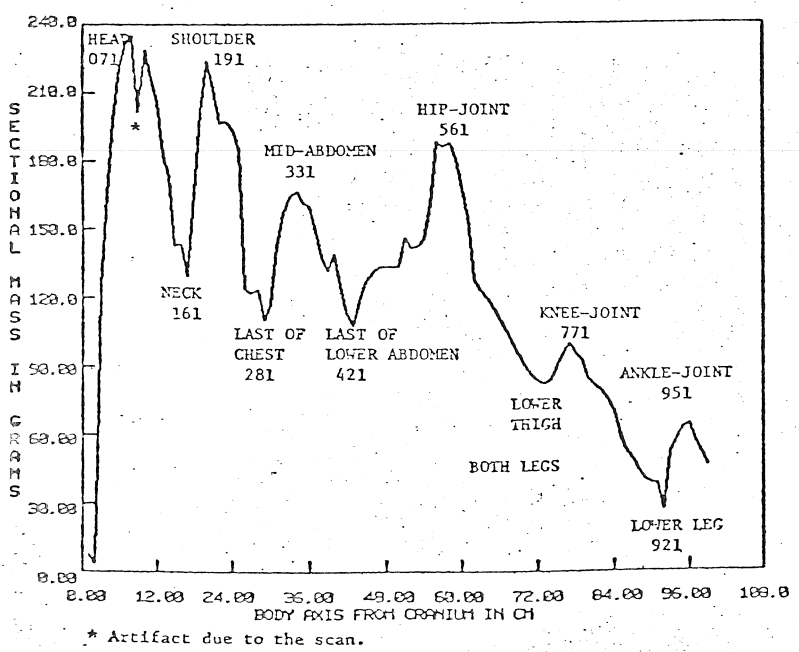

* Artifact due to the scan.

Figure 2

THREE YEAR OLD FEMALE

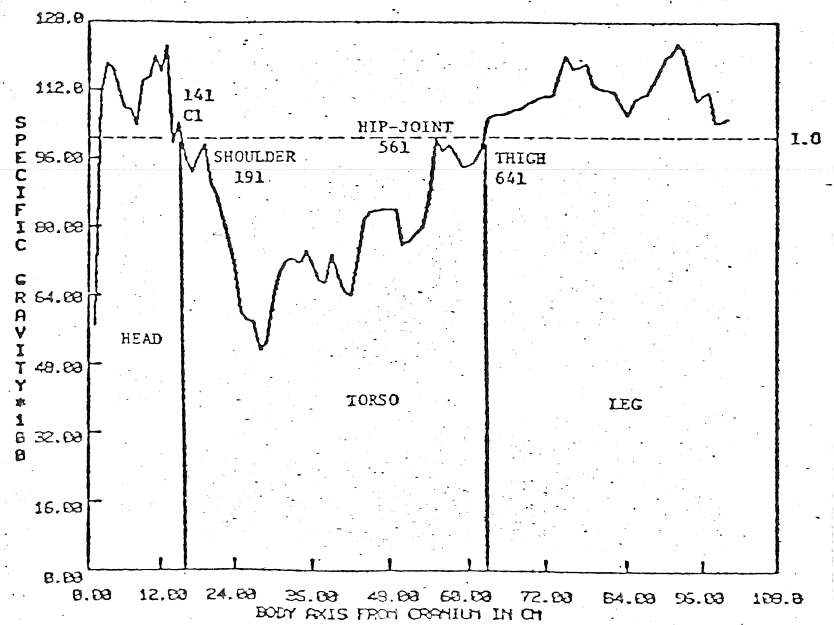

* Data from scans 081 and 921 which have artifacts have been deleted in the plot.

INFLUENCE OF THREE DIMENSIONAL GEOMETRY ON SUCCESS IN THE BENCH PRESS.

N. Madsen, Department of Mechanical Engineering and T. McLaughlin, National Strength Research Center; Interdisciplinary Biomechanics Laboratory; Auburn University; Auburn, Alabama.

The bench press motion is presently considered the most frequently used of any weight training exercise. Despite the widespread use of the bench press, there is a paucity of research on its performance. In the past few years, the increased incidence of musculoskeletal injuries in the population due to bench presses served as motivation to begin detailed analysis of this motion. Initial work involved 2D biomechanical analyses of 104 trials of national and world class powerlifters from high speed films collected at the 1974, 1978 and 1979 U.S. Sr. National Championships, 1979 World Championships and 1980 World Series. An additional twenty-six filmed trials of beginners and intermediates, as well as filmed laboratory trials with synchronous EMG records of the current world superheavyweight record holder on the bench press were also analyzed.

Kinematic studies revealed two important characteristics of the performance of high-skilled lifters. First, they clearly minimized the bar's acceleration in both descent and ascent during the lift (average peak acceleration $<1 m/s^2$). Second, there was a significant difference between the high-skilled lifters and the beginners in the sequence of movements used. This especially involved the magnitudes of the horizontal components of the motion of the bar during the lift. More sophisticated laboratory analyses were thus conducted contrasting world champions with beginners, incorporating 3D cinematographic spatial kinematics, electromyography, and musculoskeletal modeling procedures. Results indicated the existence of a "groove", or particular path that should be followed, for achieving maximal performance. Following this "groove" permitted optimal muscle involvement and sequencing (particularly for pectoralis major, anterior deltoid and triceps). Furthermore, such changes in technique were reflected in corresponding alterations in joint constraint forces, with potential bearing on injury mechanisms.

Force Interplay in Cross-Country Skiing

Hans Ekstrom, Department of Mechanical Engineering
Institute of Technology, 58183 Linkoping, Sweden

The aim of ski mechanics is, and always has been, to reduce the normal pressure and friction between man and snow. This investigation is intended to express in biomechanical terms, the diagonal stride and double-poling in cross-country skiing. Tradition and long experience have led to adjusted ski length, width, camber and weight, with respect to the skier's weight, height and skill. All types of skis have varying cross-sections, longitudinal and transversal flexibility and with a camber designed to distribute the skier's weight and maneuvering forces along the ski track in a suitable way. The bottom surface of skis work in three zones - two gliding zones and one gripping zone under the foot. In order to measure the force interplay between the skiers, ski and snow, the following equipment has been developed and used with cross-country skis and poles: camber control - adjustable 14-35mm camber height and stiffness which allows comparison tests with the bottom surface; b) measuring platform - including five force measuring calls for vertical and horizontal direction; c) strain gages - attached to ski poles for measuring propulsion; d) telemetry amplifier - for signal transmission, 3 channels; e) calibration equipment - to analyze pressure distribution of static and dynamic force; and f) portable glide testing equipment, consisting of an adjustable angle measuring device for measuring a plane surface of snow covered ski tracks. The results show the vertical and horizontal force between the skier and the skis and pole in diagonal stride and double-poling in cross-country skiing. The vertical force in each stride is dependent upon the skier's experience and the condition of the ski tracks (see table following).

Vertical Force in Body Weight (Q)

Ski-Track	Skier	
	Average	Experienced
Soft	1,2Q	2Q
Hard	1,5Q	3Q

Similarities exist between running and skiing as concerns vertical force and position of resultant force. By measuring the static and dynamic pressure distribution for a normal and a test ski with camber control, it is possible to determine which zones of the ski are active, which is especially important from the waxing aspect. There is starting and gliding friction within the stationary pause in each diagonal stride of the ski. An investigation into the start and glide friction has been conducted with glide and field test equipment.

References

Cavanagh, P.R. and M.A. Lafortune. (1979) Ground reaction forces in distance running. Submitted to J. of Biomechanics, 1979.

Dillman, C.J. and P.E. Martin. (1980) Biomechanical determinations of effective cross-country skiing techniques. Personal communications.

Waser, J.S. and B. Nigg. (1976) Film analyse biomechanisher parameter beim ski long. lang. Leistungssport 6, (1976):6 pp. 476-482.

A KINETIC ANALYSIS OF CARVED AND SKIDDED SKI TURNS

by Bard Glenne
Civil Engineering Department
University of Utah, SLC, UT 84112
and Jim Vandergrift
K2 Corportation, Vashon Island, WA 98070

ABSTRACT

Development of better ski equipment (skis, boots and bindings) has generally been more helpful in improving our skills than our knowledge of physics and biomechanics. However, scientific methods now being applied to analyze ski technique, ski instruction and ski equipment are changing this process.

In this work the external forces (active and inertial) acting on a turning skier and his or her skis are considered. The internal forces in the skis (3-dimensional bending & vibrational forces) as well as the biomechanics of the skier are not tackled here. Moreover, the air resistance forces (lift and drag), ski moments and the force due to changes in curvature are neglected.

The vector models constructed in this paper serve to explain the basic mechanics of ski turning. The models enable one to define the carved and the skidded turns and to show their relative properties and merits. The mathematical models produce values of outward forces and skier edge-setting angles which agree with observed values.

Analysis of the equations show that turning early, using a large turning radius and a small sideslipping angle are beneficial to minimize skidding and outward forces and to maximize skier acceleration. To further refine this method of analysis better knowledge of actual turning trajectories and turning velocity changes is necessary.

A good skier must match the sideslipping angle, the edge-setting angle, the ski weighting and steering to his or her strength, ability, equipment and the existing snow and hill conditions. Thus a small difference in the ability to make a ski carve rather than skid often translates into meaningful seconds in ski races.

FORCE AND POWER PRODUCTION IN THE FENCING LUNGE

Deborah L. Gebhardt, Advanced Research Resources Organization
4330 East West Highway, Washington, D.C.

In the sport of fencing the lunge is the basic component of all attacking actions that carry the point of the foil to the target. The purpose of the study was to identify the kinetic variables that discriminated between novice and skilled fencers in the execution of the lunge. The subjects were 15 male novice and 15 male highly skilled intercollegiate and Olympic fencers. A Kistler Type 9261A force platform, high speed cinematography (150 fps), an electrogoniometer, and a timing circuit were used to obtain synchronized records of each subject executing a lunge to a silhouette of the legal target area used in foil fencing. The parameters analyzed were the horizontal (X) and vertical (Z) forces and impulses, resultant force (R-force), power, and whole body center of mass (CM) displacement and velocity. The lunge was divided into four phases representing quartile measurements of the horizontal CM displacement from front foot take-off to foot contact with the floor at the end of the lunge. The beginning and termination of each phase were referred to as points one through five (e.g., Phase I was bounded by points 1 and 2). All data were normalized prior to analyzation and were tested for significant between group differences with a multivariate statistical procedure. The skilled fencers' X and Z forces at points 1, 2, and peak force were significantly greater than the novice fencers'. The skilled fencers displayed a rapid build-up of X and Z forces during Phase I, followed by a sharp decline in Phases II and III which resulted in a change in the vector direction of the X-force. The novice group did not exhibit this pattern. The skilled and novice groups R-force curve was similiar to their X and Z force curves. The vector direction of the angle of application of the R-force changed for the skilled fencers.

The total X and Z impulses for the novice group were larger than for the skilled group, due to the skilled fencers' sharp decline in force after Phase I and change in the X-force direction. Power in the fencing lunge was defined as the dot product of force and CM velocity. The power output curves for both groups were similar to the R-force and rear knee velocity curves.* The skilled fencers exhibited a large increase in power from point 1 to peak power at point 2, a pattern observed for the X, Z, and R forces. The novice group did not attain peak power until point 3.

The empirical data was reviewed to select a parameter for modeling that was crucial to performance. The R-force met this criterion and a descriptive model that accounted for the qualitative and quantitative identification of variance between groups was formulated. When the tenents of the model were met using the empirical skilled fencers' data, it was predicted that 1) the horizontal displacement of the CM was approximately 25% of the fencer's height, 2) the lunge distance was 70% of the fencer's height, and 3) upon completion of the lunge, the fencer was able to recover more rapidly to his initial position. These three predictions because of their readily accessible measurement were found to be of pratical importance when attempting to optimize performance.

* Presentation AAHPERD, April 1980.

STRUCTURAL CHARACTERISTICS OF MOTORCYCLE HELMETS+

Herbert B. Kingsbury,* Paul R. Rohr,**

Joyce E. Polecaro*

Development of mathematical and heuristic models for investigation of the relationships between motorcycle helmet structure and head injuries resulting from impact requires knowledge of the structural performance of helmets in common use. Although all helmets must comply with minimum performance standards, they differ widely in construction, material, style, price, and presumably, in the amount of protection provided to the wearer.

This paper presents the results of a series of nearly two hundred tests on one hundred and fifty individual motorcycle helmets of five different brands to determine their force-deformation characteristics and their resistance to penetration. Tests were carried out with helmets mounted on headforms in servo-hydraulic test machines. Among the test variables were point of loading (top, front, back, and sides), environmental preconditioning (-29°C, 51°C and water soak), loading rate (quasi-static to 14 m/s) and headform type.

Results presented include the measured force-deformation curves, tabulated data showing permanent change in helmet thickness, energy of deformation, secant modulus at 40 KN force, and force and deformation at which the helmet is fully crushed. Also presented are measured helmet thicknesses, weights and mass center locations.

It is concluded that loading rate and environmental conditioning have only a minor effect on helmet force-deformation characteristics. Total energy of deformation at any orientation correlates strongly with helmet thickness and substantial differences are found among the different brands and styles in energy of deformation, crushing force and total deformation at complete crushing. Fiberglass and polycarbonate shell helmets are found to differ substantially in their resistance to penetration by a sharp-pointed cone. Finally, it is shown that the protection afforded by helmets to front (forehead) impact is typically much less than that for top or rear impact. Design modifications to the helmet shell to increase forehead protection are suggested.

+Study Sponsored by The Insurance Institute for Highway Safety
*University of Delaware, Newark, Delaware
**Insurance Institute for Highway Safety, Washington, D.C.

DESIGN CRITERIA FOR ALPINE SKI BOOTS

- Howard Medoff, Javin Pierce, Malcolm Pope and Robert Johnson

This investigation is concerned with the relationship between performance, comfort and safety in Alpine ski boots. The ski boot acts as a direct coupling between the skier and the ski, transmitting control forces down to the ski. Feedback is also an important function of the boot. This is accomplished through the transmission of those forces emanating at the ski/snow interface, to the skier, via the boot.

Mechanical properties of the boot, namely forwards/backwards stiffness and lateral/medial stiffness, are important parameters in this control system. Pressure distribution in the cuff area of the boot (along the lower leg) also makes an important contribution to the "control characteristics" of the boot.

Safety aspects of this system can be related to the location of the "effective fulcrum point" on the tibia in a forward lean configuration of the boot. This fulcrum point can be obtained by a mathematical analysis of the pressure distribution inside the lower leg area of the boot. The magnitude of this force and its location can be related to the breaking strength of the tibia and a "margin of safety" can be calculated for various boot designs.

A comfortable ski boot is one in which there is no foot/leg pain during skiing. This is obviously desirable, but in practice rarely obtained. Pressure (pain) tolerance levels can be determined in various areas of the foot/leg. This information will aid in determining the potential pain levels for various boots. Time factors also play an important role in this process.

Test Methods: A ski boot stiffness tester was designed and constructed. Stiffness tests were conducted in both forwards/backwards and lateral/medial modes. Coupling effects between the two were also measured.

Pressure distribution in various areas of boots was also measured. Transducers were designed for this purpose. Tests were conducted in the laboratory as well as on a ski slope. On-slope testing was performed using a portable instrumentation system, developed for these tests.

Foot/leg "pressure tolerance level" tests were performed on a number of subjects to determine the pressure needed to cause pain in various areas of the foot/leg. A cross modality matching technique was used, correlating a measured hand grip pressure and observed length of lines, as determined by our subjects, to our applied foot/leg pressure.

Results: In forwards/backwards stiffness, for typical boots, we have found a non-linear relationship with the stiffness increasing as the dorsiflexion angle increases. Hysteresis is also present due to an inherent mismatch between the foot/leg and the inside of the boot. Similar results have been obtained in lateral/medial tests. Our pressure measurements have shown an increase in pressure as the subject cycles forward. All pressure values are in phase with increase of dorsiflexion angle.

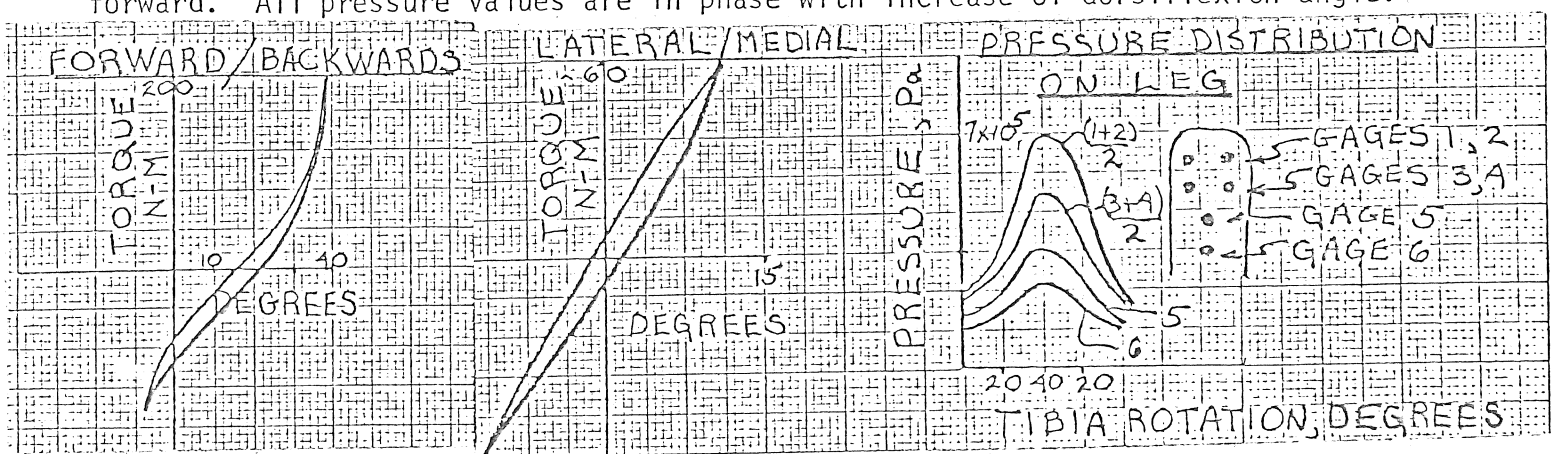

MEASUREMENT OF PEDAL LOADING IN BICYCLING

R. R. Davis
Graduate Student
Department of Mechanical Engineering
University of California
Davis, CA 95616

M. L. Hull
Assistant Professor
Department of Mechanical Engineering
University of California
Davis, CA 95616

As fossil fuel supplies diminish, alternative modes of human transport such as the bicycle are receiving greater emphasis in research and development. While bicycling is highly efficient, fatigue of the leg muscles limits the speed and distance travelled. To realize maximum utilization it is desirable to design the bicycle and related equipment so that leg muscle fatigue is minimized. In this regard, the foot-pedal connection is important because it dictates which muscle groups are available to supply motive power.

In the study of muscle group utilization, pedal loads are of interest because (1) the rider output power can be directly calculated and (2) the efficiency of the pedalling process evaluated. The objective of this paper is to compute torque and evaluate pedalling efficiency for three stages of the foot-pedal connection hierarchy outlined by Hull [1]. Calculations are based on measurements made by a new instrumentation system (see Ref. [2]) which monitors both the normal and tangential pedal loads and the absolute pedal position.

Data were recorded in the laboratory from a test subject "riding" on bicycle rollers. Rollers revolve both wheels so that the rider must balance himself just as if he were riding normally. An LSI-11/23 minicomputer with a data acquisition interface capable of 12-bit resolution acquired the data. With the left pedal instrumented, data were recorded over one complete revolution for each foot-pedal connection. Each data channel was sequentially sampled at 1000 samples/s. Resolution at 6.28 rad/s (60 RPM) was 6.3×10^{-3} rad (.36 degrees).

The efficiency plot for the lightweight shoe with toeclip and cleat is shown in the figure. Efficiency is the percentage of resultant load which produces torque and indicates how well the rider is supplying useful load to the pedal. The major conclusion is that efficiency with the cleated shoe is much better than that with the other connection. In the figure, the second peak from 190 to 240 degrees (reference is top dead center) indicates an active role of the cleat in power generation. Efficiency plots for the other connections do not exhibit the second peak. Work by the flexor muscles is made possible by the cleat. Contrary to popular belief, negative (back) shear load rather than positive (up) normal load is most important during the backstroke and upstroke. Loading plots show that the normal load almost always contributes to the negative torque during this phase. By producing the highest efficiency and alleviating extensor muscle loads, cleats minimize lower extremity muscle fatigue in bicycling.

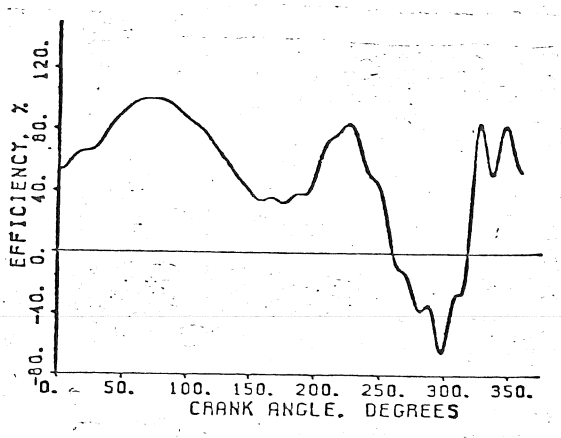

References

1. Hull, M.L., "Biomechanics of Lower Extremity Injuries in Human Powered Transportation," Proc. 6th New England Bioengineering Conf., Pergamon Press, March 1978, pp. 51-54.
2. Hull, M.L., and Davis, R.R., "Biomechanics of Overuse Injuries in Bicycling: Instrumentation," submitted for publication in 1980 Advances in Bioengineering.

77
6A

HUMAN SOMERSAULTING STABILITY: A KEY TO UNDERSTANDING HOW AIRBORNE TWISTS ARE INITIATED

Richard N. Hinrichs, Biomechanics Laboratory, Penn State University
University Park, PA 16802

A rigid body possessing three distinct principal moments of inertia cannot rotate in a stable manner about its intermediate principal axis of inertia. Anyone who has ever tossed a tennis racket into the air has seen the consequence of this instability. When you try to make the racket do a simple "somersault" about a transverse axis it will always "twist" before it comes back down. The author believes this is one mechanism used by athletes to perform twisting somersaults. The purpose of this study was to investigate this phenomenon in human somersaulting motions.

A highly skilled trampolinist was filmed while performing various somersaulting maneuvers on a trampoline. A two-camera 3-D cinematography method was used to record the locations of body segment endpoints in space. These data served as input to a series of computer programs that calculated the successive orientations of the three central principal axes of inertia (CPAIs), the magnitudes of the corresponding central principal moments of interia, (CPMIs), and the 3-D angular momentum.

The results showed that during a back layout somersault, the subject was rotating about the inherently unstable intermediate CPAI. Yet he did not twist. It is hypothesized that rotation without twisting was maintained by the subject making small corrective movements to keep the somersaulting axis essentially parallel to the angular momentum vector. These adjustments were not needed during pike or tuck somersaults because the somersaulting axis in these body positions corresponded to the inherently stable maximum CPAI.

Of special interest was the study of the airborne twisting maneuver present in the execution of a fliffis (a double forward somersault with a one half twist during the second somersault). As the first somersault progressed the maximum and intermediate CPMIs converged to a common value (see Figure 1). At this instant small deviations from body symmetry produced a marked shift in the orientation of the somersaulting axis (the maximum CPAI) away from the angular momentum vector. Thus the twist was initiated well before any visual signs of twisting had occurred and without any overt action on the part of the athlete. This provides some new and valuable insight into how airborne twisting maneuvers are initiated.

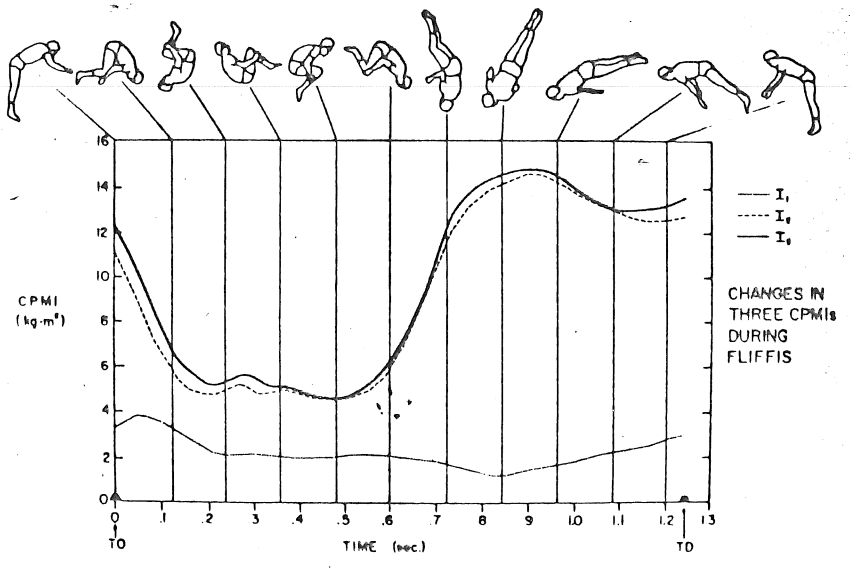

COMPUTER SIMULATION OF A FULL TWISTING DIVE

Nancy L. Pike
Department of Health, Physical Education, and Recreation
University of Houston
Houston, Tx. 77063

The purpose of this study was to develop a computer simulation of a forward, full twisting dive in the layout position. The results of this simulation would indicate whether the twisting rotation observed in a dive could be completely produced by the counter rotation of the diver's arms.

The computer program, which simulated the airborne phase of a twisting dive was developed using a 4x4 matrix transformation technique. In the diving simulation the diver's body was modelled as a system of five inter-connected spatial linkages. The equations of motion of the 12 degrees of freedom accorded the diver's body were derived using Lagrangian mechanics.

The computer program predicted the translational and angular orientation of the diver's trunk-head-legs segment during the flight phase of his dive. The input data required by the program included the diver's body segment and initial takeoff parameters, and the motion of his arms, as measured relative to his trunk-head-legs segment. The diver's initial takeoff parameters were the somersaulting angle and angular velocity and the translational velocity of his trunk-head-legs segment.

The differences in the somersaulting, rolling, and twisting angular displacements of the simulated divers' trunk-head-legs segments at water contact were explained in terms of the divers' angular momentums. Once a diver was airborne, his absolute angular momentum had to be conserved. The relative motion of a diver's arms caused his trunk-head-legs segment to experience a rolling rotation. The diver's angle of roll reoriented his body so that his absolute angular momentum, which was determined at the instant of takeoff, produced both somersaulting and twisting rotations.

Although none of the divers simulated in this research project attained the correct somersaulting, rolling, and twisting angular displacements at water contact, the computer results did indicate that given the correct takeoff parameters and arm motions, a diver could perform a forward, full twisting dive in the layout position through the counter rotation produced by his arms. The diver's final somersaulting angular displacement was a function of his somersaulting angle and angular velocity at takeoff and his time of flight, which depended upon his translational velocity at takeoff. The change in the magnitude of the diver's roll angle was due to his arms' angular velocities and the amount of twist he exhibited. The diver's final twisting angular displacement was a function of his somersaulting angular velocity at takeoff (i. e., his absolute angular momentum) and his angle of roll. For a diver to attain both a 0.0 rad angle of roll and a 6.28 (2π) rad angle of twist at splashdown, he had to hold his wrap position until he had a twist angle greater than 4.71 ($3\pi/2$) rad.

BODY SEGMENT ANGULAR MOMENTUM CONTRIBUTIONS TO SOMERSAULTING PERFORMANCE

Doris I. Miller and Mauno A. Nissinen[1],
Department of Kinesiology, University of Washington, Seattle, WA 98195.

In many jumping-type sports skills performance is judged upon body rotation as well as translation during the period of free-fall following the take-off. If air resistance is negligible and no external torques with respect to the center of gravity (CG) are encountered, the angular momentum of the athlete with respect to the CG at the instant of take-off remains unchanged during the flight. The role individual body segments play in generating this total angular momentum was the question addressed in the present study which focused on the support period of the running forward somersault.

Nine skilled collegiate male gymnasts performed two trials of a reverse lift running forward somersault tuck while being filmed at 200 fps. In addition, the somersaults of one novice using a reverse lift and one skilled gymnast using a conventional arm action were recorded for comparative purposes. Each frame of the support phase was digitized and resulting position-time information digitally filtered prior to the calculation of segmental velocities and local ($I\,\underline{\omega}$) and remote ($\underline{r} \times \underline{mv}$) angular momentum contributions.

Figures 1 and 2, derived from the best performance, illustrate common trends in the data for the reverse lift somersault. Local angular momentum played a minor role. The contribution of the upper extremities (local & remote) increased during support and approximated that of the trunk by the time the feet left the ground. Since the CG was taken as the reference point, the lower extremity angular momentum was predominantly negative approaching zero near take-off. The increase in total body angular momentum (from ~ 0 to ~ 40 kg-m-m/s) mirrored this lower extremity contribution.

The results of this study indicated that a simplified extension of the rigid body concept of angular momentum $(I\,\omega)$ to a linked $\left(\sum_{i=1}^{n} I_i\omega_i\right)$ system cannot be justified and does not even provide a useful first approximation. Remote contributions of the segments $\left(\sum_{i=1}^{n} \underline{r}_i \times m\underline{v}_i\right)$ cannot be ignored and in fact dominate the generation of the total body angular momentum. The important role of the head and trunk in producing a successful performance was evident.

---

[1] Present address: Johann Wolfgang Goethe University, Frankfurt, BDR.

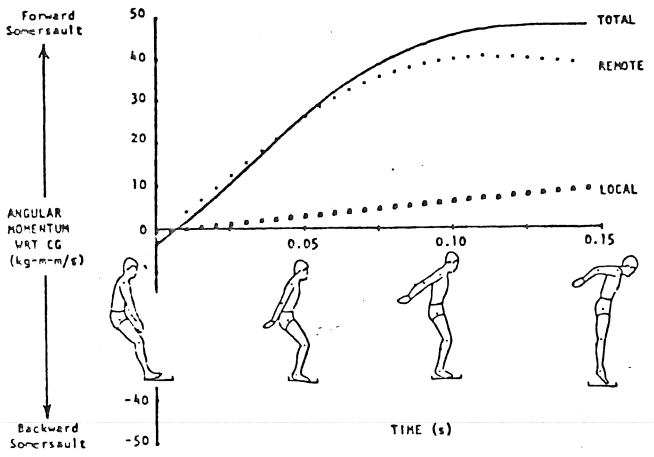

Figure 1. Local and remote contributions to total body angular momentum with respect to the CG during the support phase of a reverse lift running forward somersault tuck.

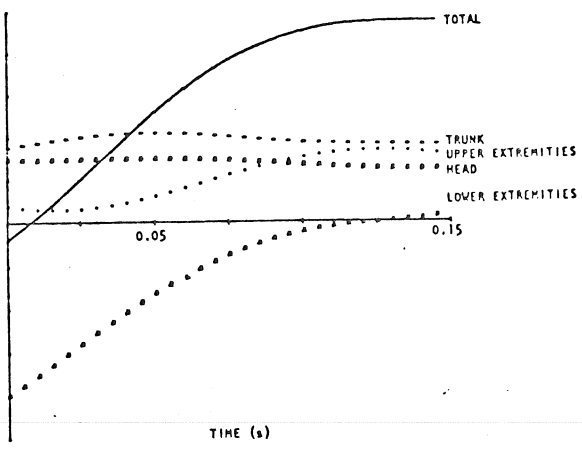

Figure 2. Segmental angular momentum-time histories with respect to CG during the support phase of a reverse lift running forward somersault tuck.

Prediction and Verification of Trajectories and Forces in the Pole Vault

M. Hubbard
University of California
Davis, CA 95616

and

D. A. Barlow
University of Delaware
Newark, DE 19711

An analytical dynamic model of the pole vault can play an important role in understanding the event and in the development and improvement of vaulting techniques. The purpose of the work reported here is to provide a more exact than any thus far, yet still tractable, model of a vaulter-pole system which will be capable of predicting the vaulter trajectory and pole forces. An additional objective is to predict the effect of vaulter muscular inputs sufficiently accurately to enable optimization studies to be performed.

The approach taken is to choose the simplest model which accounts for the primary factors involved in vaulting: large deflection of the pole and the significant effect of vaulter applied torque thereon; motion of vaulter c.m. and orientation of major body segments; work done by major muscle groups and the effect on c.m. height; the effects of varying initial conditions, pole stiffness and length, and vaulter masses and inertias; internal dynamics of the muscles to account for the fact that instantaneous changes in vaulter forces are not possible. A complete description is given in [1].

The vaulter submodel is taken to be three rigid bodies, pinned at the shoulders and hips and to the pole at the wrists, all of which move only in the vaulter saggital plane perpendicular to the crossbar. Five degrees of freedom result, x_{cm}, y_{cm} and arm, torso and leg orientations. Their five time derivatives and a first order approximation for the muscle torque dynamics ($\tau_m = 0.07$ sec for fast muscle fibre [2]) at the three pins bring the number of state equations to thirteen. The energy stored in the pole is assumed to be a function not only of end position but vaulter applied torque as well [3].

Although it was previously recognized that work is done during the vault [4], it was not possible to isolate the relative sizes of the various contributions. Computer simulations using the above model have shown that the initial kinetic energy can be augmented by roughly 20% by work done mostly by the hip and shoulder muscles [1]. An effort is presently underway to optimize the muscle time histories which may increase this muscle work.

The model has been validated by the comparison of computer simulations to experimental results from a previous study [5]. Figure 1 shows vertical and horizontal forces at the vaulting box for parameters given in Table 1. The worse agreement of the vertical force histories is felt to result mostly from the different takeoff angles. A simulation is presently being done with the exact experimental parameters.

Table 1

Parameter	Simulated	Measured
Vaulter mass Kg	75.0	71.5
pole length m	4.57	4.57
pole stiffness N-m	2022	1955
takeoff velocity m/s	8.76	8.79
takeoff angle rad	0.136	0.396

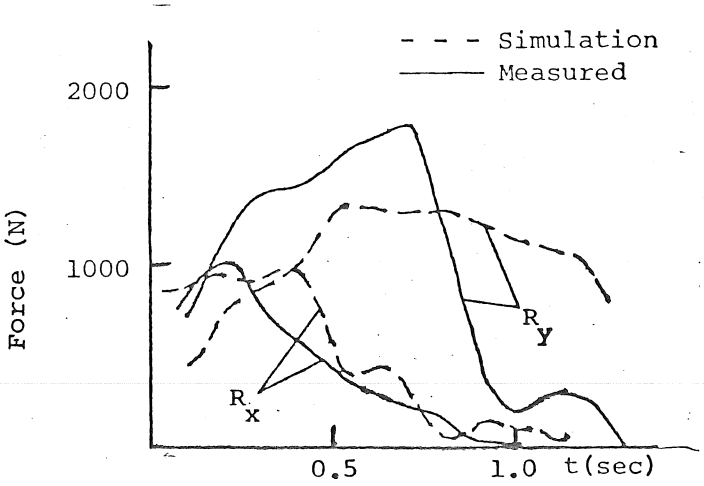

Fig. 1 Vaulting box forces

References

1. Hubbard, M. (1980), "Dynamics of the pole vault", in review.
2. Hatze, H. (1977), Biol. Cybernetics, 25, 103-119.
3. Hubbard, M. (1980), J. appl. Mech., 47, 200-202.
4. Dillman, C.J. and Nelson, R.C. (1968), J. Biomechanics, 1, 175-183.
5. Barlow, D.A. (1973), "Kinematic and kinetic factors involved in pole vaulting", Ph.D. thesis, Indiana University.

The Finger Release Sequence of Curveballs and Fastballs by College Baseball Pitchers

Joan M. Stevenson,
School of Physical and Health Education,
Queen's University,
Kingston, Ontario, Canada.

The purpose of this study was to determine the release pattern of the thumb, index, and middle fingers in releasing fastballs and curveballs. Ten pitches of each type were examined with nine right-handed college pitchers from the University of Minnesota during their competitive summer season.

The microswitches for the fingers were created with a ball, painted with electroconductive paint, and 3M electrode tape glued to finger cots and held in place with a racquetball glove. All counters of a portable six channel timer, with accuracy of 10^{-4} seconds, were initiated by the pitcher's stride onto a microswitch floor mat. The three channels used for each finger terminated as the ball was released, and the final counter stopped when the ball made contact with a microswitch in the catcher's glove.

Contingency tables, using a Pearson Chi-Square test, were used to examine various hypotheses of independence of finger release sequence for fastballs and curveballs. The results revealed that seven out of nine pitchers ($p < .05$) had the thumb coming off first independent of the pitch type. For the total pitches thrown, the thumb came off first for 96% of the fastballs and 73.6% of the curveballs. Five out of nine pitches ($p < .05$) had the index finger coming off the ball last independent of whether the pitch was a curveball or a fastball. When all pitches were examined, the index finger left the ball last in 97% of the curveballs whereas this was true for only 58% of the fastballs. In four out of seven cases, the middle finger came off the ball second dependent on the pitch type ($p < .05$). This was indicative of 72.4% of all curveballs, and 43.8% of all fastballs for the total pitches. From this data, the usual sequence of release for a fastball leaving the pitcher's hand was thumb first, followed by either the middle or the index finger depending on the pitcher. The usual pattern for the curveball, in seven out of the nine pitchers examined, was thumb off first, followed by the middle finger and lastly, the index finger.

The average velocity from finger release to catcher's glove was .5665 seconds for fastballs and .7143 seconds for curveballs. These times were similar to the average velocities of curveballs and fastballs reported in the literature. There was no significant difference within or between pitchers in the time from lead foot contact with the ground to the moment of release for fastball pitches ($\bar{x}$ = .1580 seconds), or the curveball pitches ($\bar{x}$ = .1635 seconds).

LOCOMOTION STUDIES - CAVES TO COMPUTERS

Richard A. Brand, M.D.
Roy D. Crowninshield, Ph.D.

Biomechanics Laboratory
Department of Orthopaedic Surgery
University of Iowa
Iowa City, Iowa

Locomotion has aroused the interest of man since at least the beginning of recorded history. The study of locomotion has paralleled the development of sciences in general, with philosophy, motivation, technology, and sometimes theology or politics being intimately interrelated. As in any science, advances are usually evolutionary and not ordinarilly totally attributable to a single individual; nonetheless, the citing of individual works is useful for temporally placing those advances. Our purpose is the tracing of concepts rather than an exhaustive listing of locomotion researchers. A review of this sort will necessarily exclude the mention of many important researchers; we have mentioned only those individuals who were associated with some important new concept.

The ancients understood locomotion qualitatively as patterns of body segment displacement. Aristotle developed the first systematic theory of general motion and was the first to relate such a theory to locomotion. Systematic experimentation to prove theory may be attributed to Gallileo. The concept of simplifying anatomy to study the mechanical effects of the musculoskeletal system is attributable to Leonardo daVinci. Implicit in that simplification was the idea that biologic systems behaved according to the same laws as mechanical systems. Gallileo was one of the first to submit his ideas to systematic experimentation to prove mechanical theories, thus directly advancing the science of mechanics and indirectly contributed to locomotion studies. Gallileo's pupil, Borelli, combined the ideas of his mentor and daVinci and made the first "scientific" study of locomotion of man and animals.

The availability of mechanical and photograhic devices and clocks to record and time events led to the technological advances of the nineteenth century. The works of the Weber brothers, Marey, and others provided the language by which we describe and study locomotion. The use of Newtonian mechanics to describe events associated with locomotion was the major contribution of Braune and Fischer at the end of the nineteenth and beginning of the twentieth centuries. Their use of elegant concepts and technology provides the major model for present investigations.

The twentieth century has seen major technical advances (force plates, computers, electromyograms, statistical analysis, etc.) but few major conceptual advances. Amar introduce the force plate in 1916 and Sherb the use of electromyograms to study gait in the 1940's. The latter has proven useful in temporally, but not quantitatively, defining muscle activity during locomotion. The computer has made technically possible complex schemes to mathematically predict muscle and joint forces, but these schemes have yet to be substantially validated.

Future work will refine the accuracy and validity of mathematical descriptions of locomotion and will lead to means of optimizing function in normal circumstances (i.e. athletic events) and controlling function in pathologic circumstances (i.e. paralytic gait).

THE PREDICTION OF VERTICAL IMPACT FORCE DURING RUNNING

E. C. Frederick (Department of Zoology, University of Montana, Missoula, MT 59812)
John L. Hagy and Roger A. Mann (Gait Laboratory, Shriner's Hospital, San Francisco, CA 94122)

By way of exploring the causes of interindividual variation in vertical impact force (i.e. the initial peak of the vertical ground reaction force curve) we have looked at the relationship between impact force and a number of kinematic and anthropometric variables. This analysis has provided us with multiple regression equations for the prediction of vertical impact force.

The equations were derived from data on 9 runners (6♂, 3♀) ranging in body weight from 90.9 kg. to 45.5 kg. Each runner was asked to run 5 barefoot trials across a Kristal force platform at each of three running speeds; 3.4, 3.8 and 4.5 $m.sec^{-1}$. The trials were filmed at 50 fps to give us a kinematic record, and speed was checked by two photocells positioned at head height. Individual vertical force records were analysed for the magnitude and time of occurrence of the initial impact peak. Summary data from this analysis are shown in Table I. The frame of the film record most nearly corresponding to the time of peak impact for each trial was analysed for: the angle to the horizontal of a line from the greater trochanter to the center of foot contact, the angle of foot dorsiflextion, the vertical height of the hip at contact, and the horizontal offset of the hip from the point of contact. A half stride cycle on the film record was used to measure: step length, half-stride length, total vertical excursion of the hip, and the horizontal distance travelled by the hip from patella cross to its maximum height.

Table I. Mean Vertical Ground Reaction Force and Time of Occurrence of the Impact Peak for Three Speeds of Running.

Speed($m.sec^{-1}$)	Mean Impact Force±S.E.M. (Newtons $\cdot 10^3$)	Mean Impact Force ±S.E.M.(%Body Wt.)	Mean Time of Occurrance±S.E.M. (% Contact Time)
3.4	1.365±0.118	203.4±17.2	2.44±0.65
3.8	1.590±0.169	232.9±19.6	3.71±1.12
4.5	1.963±0.182	286.3±15.9	4.64±1.39

These 8 variables along with speed, body weight, height, and standing hip height were plugged into a stepwise multiple regression program with vertical impact force as the dependent variable. The resulting equation which incorporates all variables has a multiple correlation coefficient of 0.748. Using only height, weight, standing hip height, and speed of run to predict impact force the multiple R equals 0.672. The variables that contributed most significantly to the prediction of impact force are, in order of decreasing importance: weight, speed, vertical excursion of the hip, the angle of dorsiflexion, half-stride length and step length.

These data and the resulting equations show that, on average, vertical impact force increases in a regular manner with increases in speed and with increased body weight. It is also apparent that the position of the foot at contact and various features of the mechanics of the stride are also covarying with vertical impact force. These data give us helpful clues to the causes of interindividual variation in impact shock at foot strike in running.

THE EFFECTS OF RUNNING SHOES ON RUNNERS GROUND REACTIVE FORCES

R. Strain, J. Ball, C. Stanitski, L. Micheli, J. Mansour, and S.R. Simon

Gait Analysis Laboratory
Children's Hospital Medical Center, Boston, Ma. 02115

The purpose of this study was to evaluate the effect of running shoes on runners ground reactive forces. Ground reactive forces during running have been previously measured (1,2) and much attention has been paid to running and testing of running shoes, but little has been done relating one to the other.

Experienced (>50mi/week) and inexperienced runners ran in a gait lab over two forceplates (3). Ground reactive forces were recorded (vertical, fore-aft, medial-lateral) and sampled at 500 Hz. Running velocity was measured using a photographic technique. Subjects ran barefoot and in a variety of running shoes. Analysis of the ground reactive forces was carried out evaluating overall patterns as well as fourier analysis. Shoes alone were tested for their mechanical characteristics. Subsequently comparisons of these parameters were evaluated in the same subject and between subjects.

The initial slope of vertical force vs. time was found to be higher in barefoot running as compared with any of the running shoes. Peak load of approximately two and one-half to three times body weight were consistently observed regardless of foot covering implying a force controlled system. Changes in fourier power spectrums revealed more power concentrated at lower frequencies in runners wearing running shoes. The relationship of the natural frequency of the shoes (resonance) and damping to better performance and reduced injuries are discussed.

References 1. Fukanaga, T., Matsuo, A., Yuaga, K., Fujimatsu, H., and Asahiana, K.: Mechanical power output in running. IN: Biomechanics 6/B edited by E. Asmussen and K. Jorgensen. Baltimore: University Park Press, Vol. 6B:17-22, 1978.

2. Cavagna, G.A., Saibene, F.P., and Margaria, R.: Mechanical work in running. J. App. Physio. 19:249-256, 1964.

3. Simon, S.R., Deutsch, S.D., Nuzzo, R.M., Mansour, J.M., Jackson, J.L.J., Koskinen, M.D., and Rosenthal, R.K.: Genu recurvatum in spastic cerebral palsy. JBJS Vol. 60-A No. 7 pp. 882-894, October 1978

Mechanical Energy Conservation During Human Walking

J.M. Mansour, M.D. Nowak, S.R. Simon
Children's Hospital Medical Center and
Harvard Medical School, 300 Longwood Ave., Boston, MA.02115

The purpose of this investigation was to determine changes in mechanical energy conservation and energy transfer as a function of walking speed during normal human locomotion. A three dimensional, twelve body segment energetic analysis of human walking was implemented. Special consideration was given to the need for modelling the torso as a group of segments with distributed mass rather than the concentrated point mass as commonly employed. In addition no assumptions were made to impose symmetry between right and left legs or arms, and the rotational kinetic energy of each segment was computed to determine its magnitude during walking. Five normal adult subjects were asked to walk at five different speeds ranging from what they felt was very slow to very fast. Subject displacement data during walking was obtained from digitized motion picture film.

To assess the possible interchange between the potential (PE) and kinetic (KE) energy, an energy correlation coefficient (ECC), (1), defined by

$$ECC = \tfrac{1}{2} - \frac{(\Delta KE)\ (\Delta pE)}{(\Delta KE)^2 + (\Delta PE)^2}$$

was employed. The ECC has a value of one when there is complete exchange between the KE and PE and a value of zero when no possible exchange of PE and KE exists. The ECC was computed for individual body segments as well as groups of segments. The normalized integral of the ECC over one gait cycle was computed such that an ECC of one over the gait cycle corresponded to an integrated value of one.

Of particular interest among the results was the nature of the ECC as a function of walking speed. In general it was found that at the extreme slow and fast walking speeds the ECC for the total body was lowest while at the mid range speeds it had a higher value. The exact pattern of ECC vs. walking speed was different for each subject, and in one subject the total body ECC was found to be nearly constant. A qualitatively similar pattern of ECC was found for the system composed of the torso plus arms, however, these values were higher than for the total body. Across different subjects, the normalized ECC for the total body and the torso plus arms were in approximately the same range.

The results of this mechanical energy investigation show that a more complete interchange between KE and PE may exist at some walking speeds and implies a possibly more efficient gait at these speeds. These results agree, at least qualitatively with those obtained from metabolic energy expenditure studies which have shown a minimum oxygen consumption at a certain speed within the subject's range of possible walking speeds.

References

1. Knirk, J.K. Analysis of the kinematics and energetics of the center of mass in human gait and its clinical application. M.D. thesis Harvard-MIT HST Program 1978.

Acknowledgement - This work was supported by the Rehabilitation Services Administration Grant #23-P-55854/105

Performance Indicators for Thoroughbred Racehorses*

David A. Barlow, Herbert B. Kingsbury and James D. Bray**

The purpose of this investigation was to measure and identify kinematic indicators of performance potential in the various types of quadrupedal gait patterns of thoroughbred racehorses. More specifically, a comparison was made between traditional trainer and veternarian evaluations of ability and gait parameters obtained through the use of precision motion analysis techniques.

Six Thoroughbred racehorses were filmed at Keystone Racetrack using standard high-speed cinematographical techniques. Each horse was filmed while performing walk, trot, and gallop gait patterns. The speed of the gallop ranged from 12 m/s to 16 m/s. Joint centers and body landmarks were marked with white adhesives. The kinematic data were reduced and measured using a digitizer and computer. Data were interpreted through the use of descriptive statistical techniques. Measured kinematic gait parameters included stride length and time, joint motion, sequential hoof contact patterns and overlap times, and vertical motion of the estimated centers of gravity. Shoulder-elbow cyclographs were calculated from joint motion data.

The horses were compared for each of the kinematic parameters to determine if a pattern could be found by which they could be grouped or assigned a relative ranking. These rankings were then compared with the perceived ability ranking of the veterinarians and trainers. Aspects of the overlap patterns were found to discriminate well between more and less able horses as did the sequential hoof contact patterns. Vertical motion of the mass center was not found to be a reliable measure of ability, but phase relationships between vertical motion and hoof contact pattern was. Foreleg angle at impact was found to be an inconclusive measure although this parameter has been suggested by other investigators as a possible discriminator. Substantial differences in shapes and enclosed areas of shoulder-elbow cyclographs were observed but a specific pattern or factor related to ability ranking could not be isolated. Finally, the paths of motion of the leg joints relative to the body were found to be a log spiral in agreement with postulated theory.

*This study was supported, in part, by the Association for the Advancement of Sports Potential, Unionville, PA.

**University of Delaware, Newark, DE 19711

EFFECTS OF RUNG SPACING ON THE MECHANICS OF LADDER ASCENT

D.R. McIntyre, Biomechanics Lab., North Texas State University, Denton, TX 76203; and B.T. Bates. Biomechanics/Sports Medicine Lab., University of Oregon, Eugene, OR 97403

The purpose of this study was to examine the mechanics of ladder climbing with special emphasis being placed on the effects of rung spacing and user characteristics on the ability of the user to ascend a ladder.

Twenty male subjects, selected and assigned to one of two groups on the basis of their standing heights climbed a ladder using either a lateral or four-beat lateral gait. Each subject performed three trials, each trial corresponding to one of the following rung spacings: (1) 0.305m (normal), (2) 0.203m (narrow) and (3) 0.406m (wide).

The movements of each subject during each trial were recorded on film and direct measurements were made of the temporal characteristics of the ascents. Data were also recorded of the forces exerted on two of the ladder rungs by the left hand and left foot during a selected climbing cycle.

The results of the temporal analysis on a selected cycle of the ascent revealed no significant interactions between rung spacings and subject groupings. Significant differences were found between the rung spacings for temporal parameters selected to describe the climbing cycle. The majority of the significant differences were found for comparisons involving the normal and wide rung spacings. The general finding was that longer durations characterized the cycle period and gait phases for both the upper and lower limbs for the wide rung spacing condition.

The results of a kinematic analysis showed characteristic movement patterns displayed by each limb segment during the ascents. Some of the parameters showed distinct rung spacing and subject group dependencies.

The kinetic analysis revealed that the primary role of the hands was for the maintenance of stability in a direction perpendicular to the ladder uprights and the continuance of a constant horizontal distance between the ladder and the body. The primary role of the forces directed through the feet was found to be for the vertical elevation of the body. For the short subjects group, increases in the rung spacings were accompanied by increases in the forces exerted through the hands in directions both parallel and perpendicular to the ladder uprights. For the tall subjects group the least applied parallel and perpendicular hand exerted forces were for the normal rung spacing condition. The forces exerted through the hands of the short subjects group were of greater magnitude than the corresponding forces for the tall subjects group.

Abnormalities in the temporal, kinematic and kinetic characteristics of the gait cycles were related to an increased potential for the occurrence of a climbing accident.

CORRELATION OF DEGREE OF INDUCED CONCUSSION WITH THE DEGREE OF EXCITATION OF RESONANT FREQUENCY, RESULTING FROM HEAD IMPACT IN THE STUMPTAIL MONKEY (MACACA SPECIOSA)

Researchers are in agreement that acceleration of the head has a causative relationship to concussion and other head injuries. The physical sciences contain considerable information on how the exciting of the resonant frequency of an inanimate object can augment acceleration effects, but such information is lacking in the biological sciences. Some leading investigators of head impact trauma have suggested that impacts of the head excite resonance thus leading to more severe concussive states, but no one has attempted to quantitatively determine if such a correlation does exist and if it is significant.

This study involved six female stumptail monkeys (Macaca speciosa) that were instrumented to record heart rate and respiration as the means of assessing the duration of induced concussion. Accelerometers were also mounted directly on the calvarium to record the acceleration of the head. These signals were simultaneously recorded during an impact to the frontal region. The animals were protected from fracture by individually-fitted fiberglass caps. The acceleration-time history underwent Fourier analysis in order to determine the energy level at the surrogate's resonant frequency of 1700 Hertz.

The "rise-time only" portion of the acceleration history and the "full pulse" portion were both transformed into a frequency-energy domain, and the product-moment correlation coefficients were determined to be $r=0.0024$ for the rise-time only portion, and $r=-0.2846$ for the full pulse. Neither of these correlations was significant at the 95% level of confidence.

Submitted by: John E. Kotwick
55 Amherst
Pleasant Ridge, Michigan 48069

BIOMECHANICAL ANALYSES OF LOAD LIFTING

A. Freivalds, Ph.D.*
D.B. Chaffin, Ph.D.*
K.S. Lee, MS*

Strains and sprains during lifting account for as much as sixty percent of the injuries in manual material handling tasks in certain industries. To better understand the effects of load and posture on joint torques, the motion dynamics of six subjects lifting maximum loads in four different types of containers from floor to table height were examined. Digitized stroboscopic photographs supplied joint center coordinates, force platform data provided subject ground reaction forces and the EMG from low back surface electrodes at the L_5/S_1 level indicated approximate tension levels in the erector spinae as an approximation to the compressive forces that could be expected to occur at the L_5/S_1 joint. Furthermore the data was used in a seven link biomechanical model as described at last years ASB meeting.

Containers with handles produced a faster rise time and larger peaks in the ground reaction forces. Containers without handles produced lower peaks and slower rise times, indicating more controlled movements. Container size had little effect. Smoothed and rectified low back EMG showed similar responses, having good correlation with the ground reaction forces. These records also allowed validation of low back compressive forces as calculated by the model.

* Industrial and Operations Engineering, The University of Michigan
Center for Ergonomics

SPINE SLENDERNESS AND FLEXIBILITY IN IDIOPATHIC SCOLIOSIS; Albert B. Schultz, Materials Engineering Department, University of Illinois, Box 4348; Chicago, Illinois 60680.

Scoliosis is a condition in which the spine curves to the side. The great majority of scolioses have no known cause; these are called idiopathic. Minor idiopathic lateral curves occur in about ten percent of the pre-adolescent population. In about 0.2 percent of this population, the curves get severe enough to require treatment. Minor idiopathic curves occur in girls and boys with about equal frequency; more severe curves occur about five times more in girls.

To help examine why idiopathic lateral curves in the spine might get worse, we explored possible roles of spine slenderness[1] and spine flexibility[2]. This was motivated by likening curve progression to the buckling of an elastic beam-column. Slenderness and flexibility are two factors that govern column buckling. Slenderness was measured from spine roentgenographs of 105 boys and 143 girls with structurally normal spines, and of 21 boys and 219 girls with moderate degrees of idiopathic scoliosis. Spine flexibility was measured from clinical tests of lateral bending abilities in 61 structurally-normal girls and 63 girls with moderate degrees of idiopathic scoliosis.

The slenderness data indicated that the girls had spines that were significantly ($p < 0.01$ at ages 12 through 15) more slender than those of the boys. When slenderness in the structurally-normal girls and the girls with scoliosis was contrasted, some differences appeared, but they did not do so consistently and at best only bordered on statistical significance. Spine slenderness perhaps can help explain sex differences in progression tendencies, but other factors must also have a role in progression mechanics.

The flexibility data indicated that the structurally-normal girls had significantly ($p < 0.05$) more lateral bending flexibility than the girls with scoliosis. Ability to perform the clinical bending tests probably depends substantially on the true lateral flexibility of the spine. If it does, then this finding tends to controvert current and seemingly reasonable hypotheses that idiopathic scoliosis results from excessive flexibility in the soft connective tissues of the spine.

Factors in addition to or other than spine slenderness and spine flexibility apparently have important roles in determining whether a minor idiopathic lateral curve in the spine will become more severe.

[1] With G. Andersson, D. Ciszewski, R. DeWald, S. Sorenson, D. Spencer, and R. Winter.

[2] With K. Haderspeck, G. Mattsson, and A. Nachemson.

A MODEL OF CUMULATIVE TRAUMA DISORDERS IN TENDONS AND TENDON SHEATHS

S.A. Goldstein*
T.J. Armstrong**
D.B. Chaffin ***

Tendon and tendon sheath disorders, such as tenosynovitis, tendonitis, synovitis, deQuervain's disease, and others are associated with repetitive forceful exertions of the hands and wrists. This paper describes a biomechanical model for investigations of the etiology of these disorders.

A viscoelastic model in which stress in the tendon and tendon sheaths is related to specific patterns of hand and wrist exertions is proposed. Strain response of the tendon-tendon sheath composite is described with respect to variations in magnitude, frequency and duration of hand exertions. Injury to the tendon, tendon sheath, and trochlea structures is characterized by cumulative strain or creep in response to repetitive loading. Degeneration of normal gliding function, associated with tissue microfailure, fatigue failure, or compromises in nutrient supplies, is theorized.

This model is supported by pilot studies of the viscoelastic properties of fresh tendon preparations in cadaver hands. The figure below illustrates stress relaxation during repeated application of physiological loads at 0.22 cycles/sec.

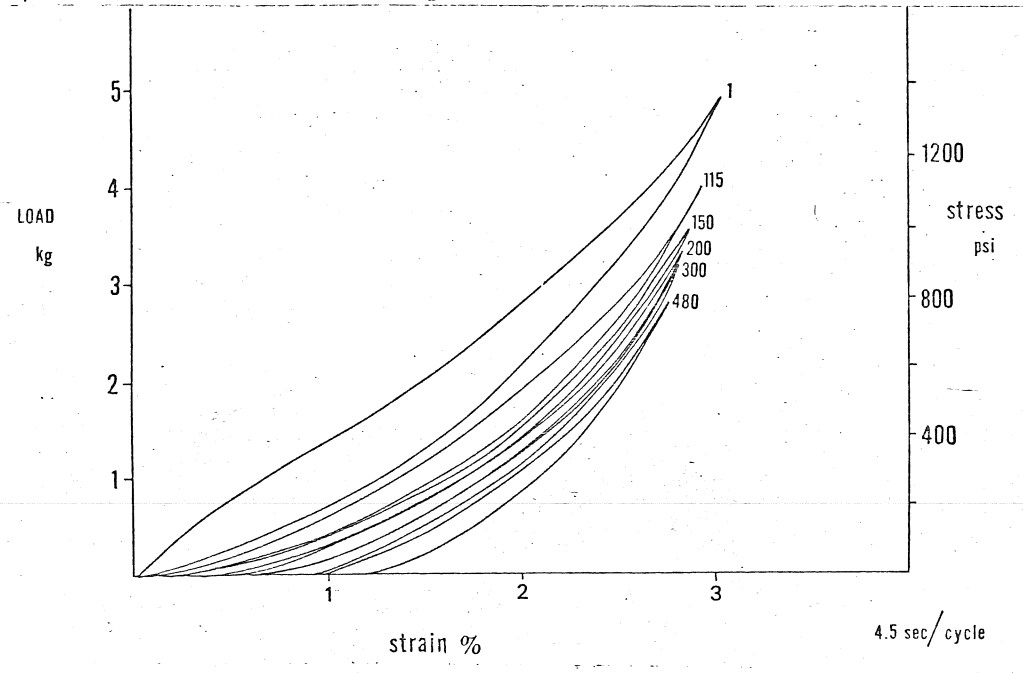

Response of unembalmed FDS tendon in cadaver hand to cyclic loading to constant strain.

* Bioengineering, The University of Michigan , Ann Arbor, MI 48109
** Environmental and Industrial Health, The University of Michigan
*** Industrial and Operations Engineering, The University of Michigan

STRAIN DISTRIBUTION ON THE LOADED PROXIMAL TIBIA

William Krause, Ph.D., Philip Ng, and Frederic Paradis, Bioengineering Research Laboratory, The Montreal General Hospital, Montreal, Quebec.

Total knee arthroplasty is a common procedure for the treatment of a number of arthritic diseases. Unfortunately, this procedure often results in the loosening of the prosthesis from the bone. The causes of loosening are unknown, but it has been postulated that loosening is the result of bone resorption due to redistribution of the stresses within the tibia. It has been shown analytically that the stress distribution on the tibia is altered due to the presence of a prosthesis. This project was undertaken to experimentally determine the strain distribution on a proximal tibia before and after the replacement with three different configurations of knee prostheses.

An intact left knee joint including the complete tibia and fibula was obtained from an amputation specimen. The specimen was cleaned of all soft tissue except for the collateral and cruciate ligaments, the capsule and the menisci. Strain gages were bonded to the proximal tibia on the anterior-medial, anterior-lateral and posterior surfaces at three levels. The uniaxial gages were placed parallel to the long axis of the tibia. The proximal femur and distal tibia were potted in PMMA for placement in a fixation jig on an Instron machine.

After establishing a baseline strain distribution for the intact loaded knee joint, a Miller knee prosthesis was implanted and the strain distribution recorded. The Miller prosthesis is a prosthesis requiring conservative resection of the tibial plateau and does not have any stems protruding down the tibia but rather four short placement stubs. Similar strain recordings were completed for a Multiradius prosthesis having a short stem and an offset hinge prosthesis with a long stem.

For an increasing compressive load up to 1500N, the recorded strain on the intact tibia increased (compression) in a linear manner. For the intact knee, the strain results showed a higher distribution on the posterior surface and a decrease in strain with distal progression. The presence of an implanted prosthesis altered the strain distribution from that of the intact knee, Figure 1. Generally, the strains measured at the most proximal level were reduced from that of the intact knee. In fact some positions were noted to be in tension. The offset hinge with its long stem revealed increased strains near the distal tip of the prosthesis.

It is concluded from this preliminary study that the insertion of a knee prosthesis causes a disruption of the strain distribution on the proximal tibia. This indicates that the normal load transmitting function of some bone is altered and could result in bone resorption and/or extensive bone remodelling and the eventual loosening of the prosthesis.

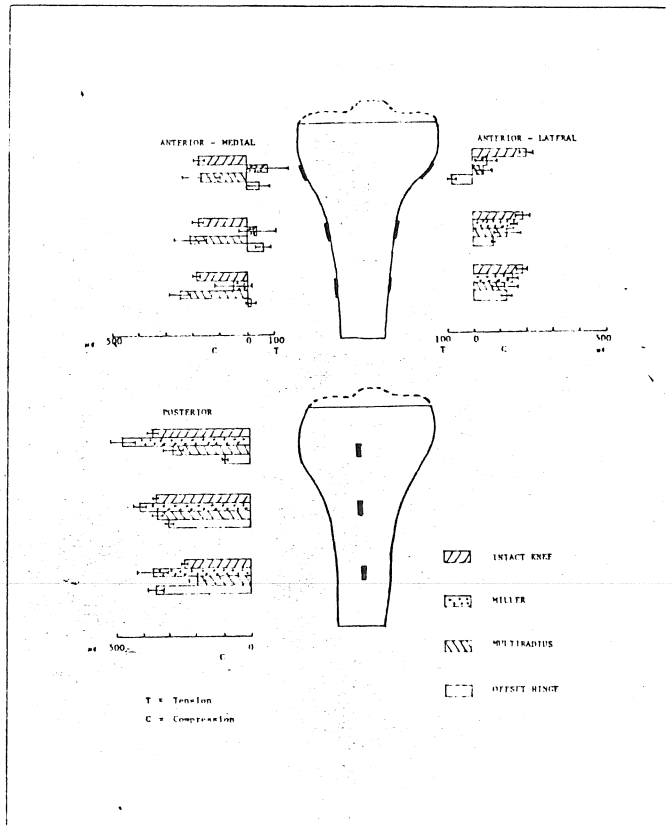

Figure 1. Strain Distribution For 1500N Load

EFFECT OF FUNCTIONAL ELECTRICAL STIMULATION (FES) ON NEUROMUSCULAR COORDINATION MECHANISMS.

J.P. Boucher and P.P. Lagassé, Laboratoire des sciences de l'activité physique, Université Laval, Québec, Canada, G1K 7P4.

This study attempted to investigate the effects of a FES training program on the neuromuscular coordination mechanisms involved in an horizontal arm sweep. Fifty male Ss, randomly allocated between a control (C), a placebo (P), a training (T), and 2 FES (S1 and S2) group, participated in pre and post-test sessions held 3 weeks apart. Groups P, T, S1 and S2 participated in 3 weeks of experimental treatment, at a rate of 3 sessions per week, interspersed between the pre and post tests; Ss of group C had no training during this period. The pre and post-test sessions were designed to assess the angular displacement and its first two derivatives, velocity and acceleration, along with EMG parameters. These measurements were taken on 5 repetitions in the pre-test session and on 2 series of 5 repetitions, 10 minutes apart, in the post-test session. Surface electrodes were placed over the motor point of the pectoralis major and the deltoïdeus anterior, two agonist muscles, and over the deltoïdeus posterior, an antagonist muscle, in order to assess their motor times and latencies. For each repetition a S had to adduct his extended right arm, suspended horizontally on a specially built apparatus, through a maximum range of 90 degrees. He had to move his limb as fast as he could through the first 75 degrees and stop the movement in the remaining 15 degrees. In every session, Ss of the T group had to execute 25 repetitions of a maximum speed horizontal arm sweep. Ss of the P, S1 and S2 groups received, on each session 25 stimulations of the 3 precited muscles. The intensity of the stimulation was 0 volt for the P group, and of 15 volts above rheobase for groups S1 and S2. The sequential order of muscle stimulation for the P and S1 group was the following: the pectoralis major was stimulated first, followed 18 ms later by the deltoïdeus anterior, and 141 ms later by the deltoïdeus posterior. This sequential order of stimulation was determined from the electromyograms of 10 Ss previously trained at the horizontal arm sweep for a period of 3 weeks. The order of muscle stimulation for the S2 group was the same for the 2 agonist muscles, but the antagonist muscle was stimulated 20 ms later than in the S1 group, i.e. 161 ms after the deltoïdeus anterior. The results of the present investigation demonstrate that limb velocity and acceleration were significantly greater ($P < 0.01$) at the post-test session for groups T, S1 and S2. The motor time of the antagonist muscle along with its latency with respect to the pectoralis major was shown to decrease significantly ($P < 0.05$) for groups T and S1, while the other latencies and motor times remained constant.

Since FES tends to improve limb velocity and acceleration and influence the fireing pattern of the antagonist muscle, the results tend to demonstrate that FES is an efficient technique to enhance learning of motor tasks which involve neuromuscular coordination mechanisms.

BIOMECHANICS OF THE CAT ELBOW IN LANDING FROM JUMPS OF VARIOUS HEIGHTS

P.A. Reback, J.L. Smith, R.F. Zernicke
Department of Kinesiology, UCLA

Although EMG analysis of landing from falls of various heights has been studied in the cat (1), parameters involved with landing from voluntary jumps have not been analyzed. This study investigates the kinematics and kinetics about the elbow joint during landing onto a force platform from voluntary jumps of heights ranging from 0.4 to 1.0 meters. Ground reaction forces and extensor EMG were recorded on FM tape. Cinematographic data were collected and synchronized via an electric pulse generator to the FM tape. Angular velocity, acceleration, and torque about the elbow were calculated for the landing phase. Rectified-average (RA) signals were measured for peak amplitude, while the untreated signals were used to establish temporal relationships between various phases of landing. Peak RA-EMG amplitude occurs 30msec prior to forepaw contact. Jump height does not appear to be a factor in angular velocity of the elbow during the landing phase (no significant difference at the α=0.05 level).

1. Watt, D.G.D. Responses of Cats to Sudden Falls: an otolith-originating reflex assisting landing. 1976. J. Neurophysiol. 36: 257-265.

DYMANIC CHANGES IN THE POWER SPECTRAL DENSITY OF MYOELECTRIC SIGNALS DURING MOVEMENT

M. H. Sherif*, R. J. Gregor**, and J. Lyman*
*Biotechnology Laboratory, School of Engineering and Applied Science, and
**Department of Kinesiology, University of California, Los Angeles, CA 90024

Myoelectric signals (MES's) have usually been considered wide-sense stationary. Recently, however, we presented experimental evidence to the non-stationarity of the signals from medial and posterior deltoids, and the medial trapezius during 90^{o} abduction of the arm[1]. We also demonstrated that suitable autoregressive integrated moving average (ARIMA) models can adequately describe the data within windows of 50 msecs duration. The analysis revealed that the patterns fall into four broad categories corresponding to the repose, mobilization, build-up and activation phases.

It is possible to derive the transfer function of the ARIMA models during various parts of the contraction[1]. The two-sided spectral density funtion of the signals from the medial deltoid during activity can be then simulated.

The plots of these simulated spectral densities are given in Figure 1. Figure 2 contains sketches of the results of the power spectral density (PDS) computations on the data collected during a given contraction, for the following cases: a) 100 msecs in the beginning of build-up phase, b) 100 msecs in the end of the build-up phase and c) 800 msecs in the activation phase. The densities were estimated with the program BMD03T of the BMD package[2] and cross-checked with the procedure SPECTRA designed at the Statistical Analysis System (SAS) Institute, Inc.

The general patterns of the two figures indicate an increase in energy concentration at low frequencies with the progression of the movement. The differences between the curves can be explained by: a) the removal of the data mean and subsequent smoothing, which produces a non-zero density at the origin and shifts the spectrum to the right so that a false peak appears[3] and b) in the activation phase, the wide variation of the white noise variance violates the assumption of stationarity for which the program was designed. The most plausible reason for the increase of evergy at the frequencies less than 80 Hz in the activation phase is that the interference of many motor units potentials results in slower variations in the waveforms. Some "synchronization" and/or "fatigue" can be also postulated.

1 Sherif, M. H., R. J. Gregor, and J. Lyman, "Statistical modeling of myoelectric signals", 1980 Joint Automatic Control Conference, August 13-15, 1980 (In Press)

2 Dixon, W. J. (ed.), BMD Biomedical Computer Programs, University of California Press, 1977.

3 Hamming, R. W., Digital Filters, Prentice-Hall, Englewood Cliffs, New Jersey, pp. 217-218, 1977

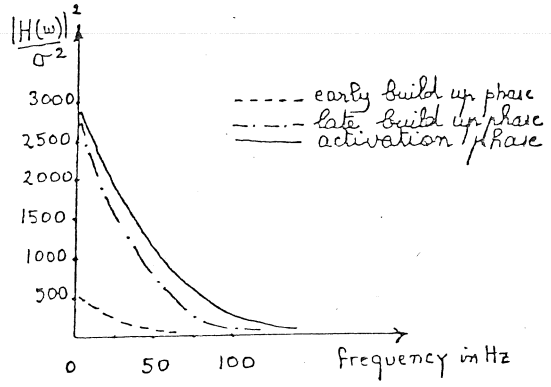

Figure 1 Simulated power spectral density for medial deltoid

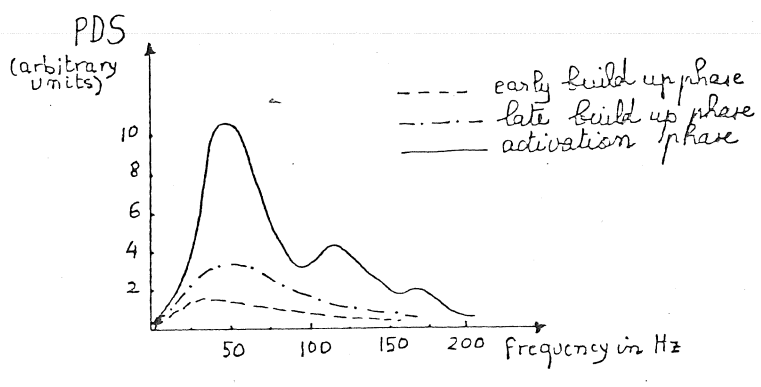

Figure 2 Computer power spectral density for medial deltoid

EMG and Electrogoniometric studies of dorsiflexors

Venkateswara Rao, D.L., Venkatappaiah, B., Ramanathan, N.
Biophysics Laboratory, Central Leather Research Institute,
Adyar, Madras 600020, India

and

I.S. Shanmugam, Professor of Physiotherapy, Artificial Limb Centre, K.K. Nagar, Madras, India.

Study of the function of muscles in the various parts of the body is of much importance. The whole body is borne by the feet, which serve as wheels in locomotion. The muscles in the lower extremity help for the stability in standing as well as in walking. The muscles which act around the ankle joint are helping the man to walk and run comfortably without causing any damage to the foot. The main dorsiflexors, namely, Tibialis anterior, Extensor Hallucis longus and Extensor Digitorum Longus save the foot from impinging the ground against the gravity and allows smooth and comfortable heelstrike. Although the functions of these muscles are known during different phases of walking, the variation of the potentials as the angle of dorsiflexion varies is not known. So, an attempt, to study how the muscle potentials vary with the angle of dorsiflexion at the ankle and the metatarsophalangeal joint, is made in this investigation.

A double channel storage myograph (MDM30 ECIL, India) has been made use of. Silver discs of 13 mm diameter were used as surface electrodes. The muscles studied were Tibialis anterior, Extensor Hallucis Longus and Extensor digitorum Longus which are the dorsiflexors. The variation of potentials at different angles of dorsiflexion at the ankle joint and the metatarsophalangeal joint was studied. The variation of the dorsiflexion angle is recorded with the help of a miniature electrogoniometer designed for the purpose in a single pen recorder. The potentials developed during a period of 100 mSec. were photographed. The integrated areas under the individual patterns were determined and the areas in arbitrary units were plotted against the angle of dorsiflexion. The potentials were studied during sitting with the knees kept exactly perpendicular to the ground. This was repeated during standing erect.

Figure 1 shows typical EMG patterns at various angles of dorsiflexion. Figures 2,3 and 4 show the areas plotted against the angle of dorsiflexion. It could be seen that the variations of the potential increase are rapid at the larger angles of dorsiflexion. The pattern is almost the same for all the three dorsiflexors. It is observed that the trend is same irrespective of slight variation in the level of the potentials. It is also observed that there is a delay for the Tibialis anterior to act while at dorsiflexion standing and dorsiflexion sitting at MTP joint.

The maximum angle of dorsiflexion varies for each individual. The Tibialis anterior reaches the maximum contraction only at the maximum limit of dorsiflexion but not before. In the case of EHL, it is observed that the muscle potential during dorsiflexion at the ankle joint during sitting is less than that during weight bearing. In the case of EDL also, the trend appears to be similar to that of EHL.

TA does not show activity till the MTP joint is dorsiflexed to about 0 degrees for sitting and about 6 degrees for standing. But, at ankle joint even the initial activity level is very high and increases fast compared to the other muscles.

MOTOR CAPACITIES OF THE CHRONIC SPINAL CAT: TREADMILL LOCOMOTION

R. F. Zernicke, J. L. Smith, C. Sabin, M. G. Hoy, and N. Meyerott
Department of Kinesiology and Brain Research Institute
University of California, Los Angeles, California 90024

For over a century there have been descriptions in the literature of chronic spinal animals, with low thoracic or high lumbar transections that were able to weight support on their hindlimbs (1). Grillner (2) has done pioneering work with exercising spinal kittens on a treadmill and has provided important information about some of the locomotor capacities of chronic spinal cats which had been cordotomized as kittens and then exercised. Our study extended the previous work to assess the influence of exercise and the age of spinalization on the locomotor patterns of the chronic spinal cat. Cats with spinal cords transected (T12-T13) at either 2 weeks or 12 weeks of age were separated into exercise or non-exercise groups. The exercise groups were fitted to a thoracic vest which was attached to upright supports on a small treadmill and the hindlimbs were placed on the moving belt while the forelimbs were supported on a platform and did not participate in the exercise. Daily training sessions of at least 30 minutes at treadmill speeds of from 0.2 to 2.0 m/s, at graded increments, were used. At 4 to 6 months post-spinalization, the locomotor patterns of the hind limbs of the exercised groups were documented with 16mm cinematography. Only the two exercised groups were filmed as the non-exercised were not able to walk on the treadmill. Kinematic data were obtained by digitizing the coordinates of the joint and limb markers. Joint coordinate data were smoothed via spline or digital filter techniques and from the displacement-time data, the limb angular velocities and accelerations were computed. Paw contact patterns, interlimb temporal patterns, and gait conversions (walking & galloping) were determined with methods similar to those reported by Wetzel and Stuart (3). Characteristics of the step cycle were analyzed with the traditional Philippson (1) step cycle and angle-angle plots (Fig. 1). The exercised animals evidenced coordinated variations in the gait kinematics with increases in the speed of walking. Gait conversions were found, and yet significant alterations in the normal phases of the walking pattern were noted; for example the E2 (yield phase) of the step cycle was absent in the stance portion.

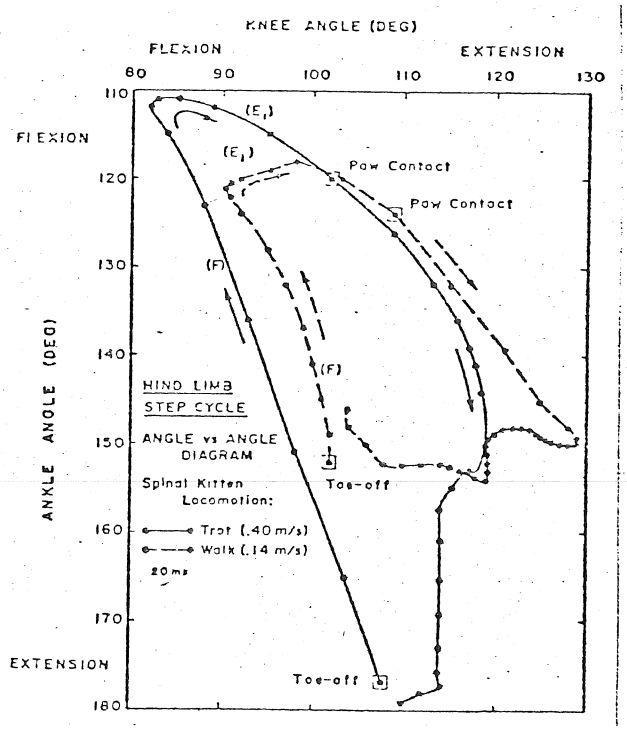

References:

1. Philippson, M. Trav. Lab. Physiol. Inst. Sovay, Bruxelles. 7 (1905) 1-208.

2. Grillner, S. In: Stein, R.B. (ed.) Control of Posture and Locomotion. New York, Plenum Press, 1973.

3. Wetzel, M.C. and D. G. Stuart. Prog. Neurobiology. 7 (1976) 1-99.

62
58

A TAXONOMY AND COMPARISON OF DATA SMOOTHING AND FUNCTION APPROXIMATION METHODS

Lebert R. Alley, Ph.D., and
James L. Smith, Ph.D.
Assistant Professors
Department of Industrial Engineering

P.O. Box 4130
Texas Tech University
Lubbock, TX 79409

Biomechanics researchers have been describing a growing repertoire of methods for smoothing and approximating biomechanical laboratory data and analytic functions. Some examples of these methods are; splines, exponential smoothing, finite differencing, Chebyshev least squares plynomials, and certain digital filters. The "quality" of performance for each of these methods is highly dependent upon two major factors.

First, the characteristic faults or idiosyncrasies of the data or function to which the method is applied will conform only partially to the particular strengths and weaknesses intrinsic to the method being applied. Examples of such complications are random noise in lab data, and spikes or discontinuties in analytic functions. Secondly, the specific criterion for measuring performance quality will change, depending upon the details of the ultimate research hypothesis or question (e.g. maximum spinal force) being persued.

This paper and presentation summarizes five principal results of a recently completed research project:

1) Taxonomy of Data Smoothing Methods - A comprehensive, structured classification scheme for characterizing the unique function and mathematical basis for data smoothing and approximation methods.
2) Repertoire of Data Smoothing Methods - A collection of the several more commonly reported data smoothing and approximating methods from the biomechanics research literature, summarized in the context of the comprehensive taxonomy above.
3) Benchmark Performance Criteria - A collection of several standard measurement criteria are proposed for evaluating smoothing performance such as: measure of smoothness on a discrete lattice, smallest maximum (minimax) deviation, and spectral density function.
4) Taxonomy of Data Faultiness Characteristics - The intrinsic strengths and weaknesses of the several smoothing methods leads to the definition of a classification scheme and data base of "challenging" test data and functions.
5) Results of Comparison of Data Smoothing Methods - The several smoothing methods are ranked according to performance for each combination of "faulty" (e.g. noisy) data, paired with a particular performance criterion.

Many of the smoothing methods, data faultiness characteristics, and performance criteria described here have been referred to in previous work. The distinguishing feature of this research has been the comprehensiveness and uniformity of the evaluative comparison of smoothing methods, under well defined and controlled conditions.

No smoothing or approximating method is uniformly best. A method's performance quality depends upon the experiment's particular data and purpose. These research results will help biomechanics experimenters characterize their data and define their smoothing performance criteria in a logical structure, to aid in selecting the most suitable smoothing or approximation method.

A Technique For Measuring Force-Position-Velocity Relationship During Jumping Movements

David F. Enzler and A. Dainis

Department of Physical Education
University of Maryland
College Park, Maryland 20742

A method utilizing a two segment electrogoniometer system in conjunction with a force platform and a minicomputer has been developed to rapidly measure force and position of the whole body center of gravity during jumping movements. The electrogoniometer system operates in the sagittal plane and is capable of measuring the two dimensional coordinates of its free end which is attached to the waist of the subject. The difference between the center of mass position and the end of the goniometer system was computed through photo-analysis and the correction function applied throughout the movement to obtain the center of mass location. A PDP 11/34 minicomputer was programmed to sample and convert to digital form the output of the potentiometers and force platform, carry out the necessary differentiation, normalize the data for each subject's height and weight, and graphically display the results. The goniometer system was found to be accurate to within .5%. The technique was applied in an investigation of the vertical jump. Different volocities throughout the take-off were achieved by varying the starting position of the subjects, and data from different trials enabled force-position-velocity and power-position curves to be generated for each individual. Results from a variety of subjects are presented. A knowledge of force, position, and velocity relationships should be helpful in understanding activities where the timing of the jumping action is required to vary with the nature of the take-off surface. Such information could be helpful in the design and modeling of take-off surfaces such as diving boards, trampolines, and mats for gymnastics exercises. The immediate display of position and velocity of center of mass, as well as the power generated, is an attractive alternative as compared to the delays involved in analyzing cinematographic records.

"An Optimization Approach to Selection of Body Segment Parameters", by C.L. Vaughan and J.G. Andrews, Biomechanics Laboratory, Department of Physical Education, University of Iowa, Iowa City, Iowa 52242.

The selection of body segment parameters (segment mass m_i, segment mass moment of inertia I_i, and center of mass location as a proportion p_i of segmental length) is a crucial aspect of many biomechanical studies. The most common approach is to use data from cadaver studies, since direct measurement of the human subject is very often impracticable if not impossible. While such an approach is convenient, the magnitude of the errors involved is unknown. The purpose of the present paper is to present an alternative method, which is based on mathematical non-linear optimization theory, for selecting m_i, I_i and p_i.

When the human body performs various movements with an open-loop configuration (i.e. with the body airborne or with a distal point of a single extremity in contact with an external reference frame), it is possible to measure the kinematics and hence calculate the forces and torque (F_{Xk},F_{Yk},T_k) at the distal point for each time k. Under such conditions, the following problem may be formulated in order to select the optimal set of body segment parameters: Given the design variables

$$b_j = \{m_i, I_i, p_i, F_{Xk}, F_{Yk}, T_k\} \qquad i = 1,14;\ k = 1,N$$

minimize the objective function

$$J = \sum_{k=1}^{N} \{(F_{Xk}-F'_{Xk})^2+(F_{Yk}-F'_{Yk})^2+(T_k-T'_k)^2\}$$

subject to certain constraints. The primes in the objective function J denote measured quantities, and N is the number of time intervals over which the optimization takes place. The equality constraints are based on (a) the principles of linear and angular momentum which are algebraic and non-linear in the design variables b_j (b) summation of segmental masses m_i equal to total body mass and (c) parameters on the left and right sides of the body are equal (bi-lateral symmetry). In addition, inequality constraints are formed by placing upper and lower bounds on the body segment parameters. Implicit in this procedure is the assumption that the "best" method has been chosen for smoothing and differentiating the raw displacement data.

To test the above procedure, three activities were chosen: running, long jumping and kicking. A Locam motion picture camera operating at 100 fps was used to gather the kinematic data, while a Kistler force plate recorded the distal extremity kinetics. The quintic spline was chosen to smooth and differentiate the raw data since it had been shown to yield satisfactory results for the acceleration of an object falling in the earth's gravitational field. The gradient projection algorithm was implemented for the optimization process and the resulting body segment parameters were found to be different from values derived using the regression equations of cadaver and other studies. Furthermore, there was a marked decrease in the objective function which resulted in close agreement between the calculated and measured kinetics.

The optimization approach to selection of body segment parameters appears to have considerable promise. However, if the activity under investigation is <u>not</u> open-loop, some time would be required to gather the extra data. Nevertheless, it is felt that the results of the present study have sufficient validity to encourage further development of the method in the future.

A Scanner for Evaluating Seating Pressures in Paraplegic Patients

Rajesh G. Narechania and Denis S. Drummond

Division of Orthopedic Surgery, University of Wisconsin Hospital, Clinical Science Center, Madison, Wisconsin 53792

Paralytic patients with scoliosis and pelvic obliquity develop a shift in the center of seating with imbalancing of trunk. In addition, there is an uneven distribution of pressure in the seating area. Because of these two sequellae, unsupported sitting may be impossible and the risk of pressure foci in the seating area with decubitus ulceration is increased. The latter complication occurs particularly in patients with absent sensation over the buttock and sacral area.

This paper reports on the design and development of the instrumentation to (1) simultaneously measure multiple pressures in the seating area thereby determining any shift in the center of seating which unbalances the trunk and (2) detect foci of increased pressure which can lead to ulceration. The objective is to quantitatively map the pressure contours in the seating area of normal children and adults as well as paralytic patients with scoliosis, fixed pelvic obliquity and trunk imbalance.

Method:

Special strain gage transducers are fabricated and laid in 8 X 8 matrix over a flat aluminum sheet 0.64 cm thick. The distance between each sensor is 3.81 cms. The outputs from the sensors are connected to the Data Translation, Data Acquisition System which has a gain of 1000 and a sampling rate of 3.7 khz. The Data Acquisition System boards are hooked up to the backplane of LSI-11/02 mini computer. The instrument operates completely under software control. The first run command scans each channel 20 times and also asks the patient to sit on the scanner. When the patient sits on the scanner and is ready, he is asked to stop the breath for a second and the new run command scans each channel another 20 times, subtracts the reading from the individual channels of the initial reading and prints the result in 8 X 8 matrix on the printer.

Results and Discussion:

The method of analysis includes: (1) the quantitative measurement of the seating pressure distributed over the seat, (2) the identification of foci of increased pressure, (3) definition of the center of seating, (4) correlation of pelvic obliquity and deformities of the trunk to changes of pressure in the seating area, and (5) abnormal shifts in the center of seating.

It is our hope that this information will objectively help in the design and fabrication of seating or those which minimize pressure foci and thus prevent decubitus ulcers in paralyzed patients (many of whom have absent sensation). This should provide for an improvement in their rehabilitation. We also hope to objectively study our indications for surgical connection of fixed pelvic obliquity and develop a method to evaluate the results from each surgery.

APPLICATION OF ULTRASONIC VELOCITY MEASUREMENT AND CAPACITIVE PRESSURE DISTRIBUTION MEASUREMENT IN GAIT ANALYSIS

Ewald M. Hennig, Biomechanics Laboratory, Pennsylvania State University, University Park, Pennsylvania 16802

Two innovative measuring devices for biomechanical investigations will be presented, which in combination provide instantly available data of kinemetric parameters and for gait analysis can register the time-dependent distribution of force under the foot.

When an acoustical transmitter is moved relative to a stationary receiver, a frequency is recorded on the receiver, that is dependent on the velocity of the transmitter. This phenomenon, called acoustical Doppler-effect, enabled us, to build an electronic device for the direct registration of the kinemetric parameters velocity, displacement (by integration) and acceleration (by differentiation). As the transmitter is very small (m = 20 g) it can be easily attached to different parts of the body without impeding the movement. There is no wireconnection necessary between transmitter and receiver and a range of up to 50 m can be obtained. A three channel device (with different frequencies) was used for registration of the movement of ankle, knee and hip during walking.

In flexible capacitive type force-transducers the mechanical-elastic and electric characteristics of special foam-rubbers as dielectrics provide a linear relationship between the mechanical force on the capacitor and its change in capacitance. Because of the low costs in material and simple manner of construction, normal-force transducers can be built from seizes of less than 1 cm^2 to several m^2 very cheap. For gait analysis a station with two force platforms (150 cm x 30 cm) was built, in order to register the vertical force of each seperate leg during walking. A capacitive sole was constructed in order to control the dynamic loads of patients during walking after lower extremity surgery. Arranged with a biofeedback instrument, an acoustical signal appears, when there is an overload on the leg and a different acoustical signal appears, when the load is too small. By means of crutches, the patient uses this instrument to adapt his movement in a manner that he walks by dynamic loads, which are not dangerous but are big enough to provide a quick recovery process.

Because of the low material costs, flexible pressure distribution mats with several thousand transducers can be built up easily. The capacitors are not formed by seperate plates, but by intersections of alongside and across running conducting stripes on both sides of the rubber mat. By multiplex-technique each single element is measured and values are stored in a computer. Besides measurements during walking and high jumping under the foot, this measuring principle was used for measurement of the pressure distribution in the prothesis-shaft of above knee amputees. A flexible shaft was especially constructed for the change of its shape, in order to see the influence of the shaft form on the pressure distribution pattern during walking.